

# **Calculation and Simulation of Generator Protection Relay Settings at Hydropower Plants**

Henrik Damlin

Master's thesis  
Supervisor: M. Sc. Ville Mäkikyrö, VEO Oy  
Examinator: Prof. Margareta Björklund-Sänkiaho  
Energy Technology, Vasa  
Study programme in Chemical Engineering  
Faculty of Science and Engineering  
Åbo Akademi University  
June 9, 2022

## **ABSTRAKT**

Vattenkraft är en förnybar energikälla där grundidén är att omvandla energin från de forsende vattenmängderna till elektrisk energi. Fenomenet kallas elektromagnetisk induktion, vilket uppstår i generatorer.

Generatorerna bör skyddas mot farosituationer som kan uppstå genom bland annat kortslutningar, jordslutningar eller överbelastningar. Generatorerna skyddas idag med digitala skyddsreläer, vars inställningar bör ställas in med ytterst noggrannhet för att säkerställa en trygg och optimal drift.

I detta arbete har det undersökts vilka standarder, regler, formler, och krav som bör tas i beaktande då inställningarna av skyddsfunktionerna i reläerna ställs in.

Simuleringsverktyg har även testats och jämförts för att kartlägga ifall något av alternativen skulle vara lämpligt för VEO Oy. Alternativen som inkluderades i arbetet var Powerfactory Digsilent, ETAP och Siemens PSS/CAPE.

Simuleringsverktygen inkluderade simuleringar och beräkningar för kraftverk och nätverkssystem, och det undersöktes hur värdefulla och användbara olika simuleringar var med tanke på inställningen av skyddsfunktionerna.

**Nyckelord:** Vattenkraft, generator, skydd, simulering

## **ABSTRACT**

Hydropower is a renewable form of energy, where the main idea is to convert the energy stored in the flowing water to electrical energy. The process is called electromagnetic induction, which is created inside a generator.

The generators must be protected against situations where faults may occur due to short circuits, ground faults, or overloads for instance. Digital protection relays are used today to protect the generators against these faults in order to ensure a safe and optimal operation of the power plant.

In this thesis, it was studied which different standards, rules, equations, and demands apply when determining the settings for the protection functions.

Simulation software have also been tested with the goal to map if any of the candidates would fulfill the needs and requirements of VEO Oy. Simulation software included in the thesis were Powerfactory Digsilent, ETAP, and Siemens PSS/CAPE.

The simulation software included different simulation and calculation tools for power plants and distribution networks. These tools were studied and evaluated whether they would be valuable and useful considering the determination of the protection function settings.

**Key words:** Hydropower, generator, protection, simulation

# TABLE OF CONTENTS

ABSTRAKT .....	I
ABSTRACT .....	II
TABLE OF CONTENTS .....	III
ACKNOWLEDGEMENTS .....	V
1 INTRODUCTION .....	1
2 THEORY .....	3
2.1 Hydropower .....	3
2.1.1 Hydropower statistics .....	5
2.1.2 Hydropower turbines .....	7
2.1.3 Pumped Hydroelectric Storage .....	9
2.1.4 Dams .....	11
2.1.5 Economical aspects regarding hydropower .....	13
2.1.6 Affects of climate change on hydropower .....	14
2.2 Generators .....	16
2.2.1 Synchronous generators .....	17
2.3 Generator protection functions .....	18
2.3.1 Stator ground fault .....	21
2.3.2 Thermal overload .....	23
2.3.3 Rotor ground fault .....	28
2.3.4 Overcurrent .....	30
2.3.5 Under-impedance .....	32
2.3.6 Differential overcurrent .....	34
2.3.7 Current unbalance .....	39
2.3.8 Under-excitation .....	41
2.3.9 Over-excitation .....	46
2.3.10 Undervoltage .....	47
2.3.11 Overvoltage .....	48
2.3.12 Frequency .....	49
2.3.13 Reverse power .....	52
2.3.14 Shaft current .....	53
2.3.15 Out-of-step, pole slip .....	54
2.3.16 Breaker failure .....	55
2.4 Generator protection relays .....	56
3 MATERIAL AND METHODS .....	58
3.1 Simulation software .....	58
3.2 Simulations .....	60
3.2.1 Powerfactory Digsilent .....	60
3.2.2 ETAP .....	64

3.2.3	Siemens PSS/CAPE .....	68
4	RESULTS.....	72
5	DISCUSSION .....	76
6	CONCLUSIONS AND RECOMMENDATIONS.....	77
	SVENSK SAMMANFATTNING .....	78
7	REFERENCES.....	81
	APPENDICES.....	84

## **ACKNOWLEDGEMENTS**

VEO Oy, the company in Vaasa region suggesting this thesis, has given me the opportunity for this master's thesis as a part of my studies at Åbo Akademi Energy technology program. I would like to thank my supervisor Ville Mäkikyrö for his support and expertise through the project. I am grateful for being able to do a thesis with such an interesting subject.

I would also like to thank Professor Margareta Björklund-Sänkiaho from Åbo Akademi for the support and valuable guidance along the way.

Special thanks also to my family and friends for their support during my studies.

Vasa, June 9, 2022

Henrik Damlin

# 1 INTRODUCTION

In this section, the background and purpose of the study is described.

Hydropower is a source of renewable energy that is used worldwide. The power generation from hydropower is expected to grow by 3% until the end of 2030 (IEA, 2020). The global generation in 2030 would double the size of the generation in 2000, if the expectations would be met.

The mechanical forces of the flowing water streams are generated to electrical energy via generators at the power plants. The generators then transfer the electricity to the power grid via transformers, which transforms the voltage levels to match the needs at that certain location. The generators can be affected by faults due to different reasons and must therefore be protected to avoid the generator and its surrounding equipment to suffer from damage and to ensure safe operation.

The protection device used is called generator protection relay. These can be programmed to protect the machine from different kinds of faults. The protection relays are set to have certain levels to trigger alarm and trip signals for the data measured. The settings in the relays must be calculated with the highest carefulness to make sure that the generator can operate securely.

VEO Oy currently delivers electrification solutions to hydropower plants mainly to Finland, Sweden, and Norway. The calculation of the settings for the protection relays is mainly aimed for the Finnish power plants, but also for Swedish and Norwegian power plants as well to some extent.

To get a better grasp around the subject, past hydropower projects are used as reference in the thesis. For different generators and power plants, different protection relays and settings are demanded. To avoid unnecessary extension of the study, only the most common variations of relays and their settings will be considered in the thesis.

The thesis will also include tests of different software used to perform the simulations, and finally a comparison of the candidates to evaluate the properties and functionality of the different simulation software. Economical differences will not be covered in the thesis, as the focus is entirely on the technical side.

The goals of the study are to collect data and increase the knowledge regarding the setting phase of the protection relay functions, and to study which simulation software would be most suitable for the company's needs.

Finally, based on the results of the study, the company will evaluate the different software options and consider a possible license purchase of the most suitable one.

## **2 THEORY**

In the following section, theory regarding hydropower, generators, and their protection functions will be covered. The theory behind the calculations of the settings for the protection relay will also be covered in detail.

### **2.1 Hydropower**

Hydropower is a source of renewable energy. The main idea of power generation of this kind is to utilize the massive forces from the water flow to create a mechanical energy in the turbine. The mechanical energy in the turbine is in the form of a rotational motion. The turbine and the rotor inside the generator are connected via a shaft. This means that the rotation in the turbine also forces a rotation in the rotor, which then creates a magnetic field in the generator (Breeze, 2018), which will be discussed later in the thesis.

Hydropower is widely distributed worldwide, and in most parts of the world, hydropower potential is found. The most advantage of hydropower has been taken in China and many South American countries. According to Breeze (2018), these areas still have much hydropower capacity unused, while in Africa for example the hydropower section is heavily underdeveloped.

The development of hydropower projects has its difficulties, since environmental aspects can often come in the way of new power plants. These problems occur mainly with the construction of major power plants, since projects of that kind are often extremely disruptive (Breeze, 2018). The major hydropower projects also demand sensitivity and carefulness, which causes even more challenges for the project development.

The development of projects concerning large power plants, which involves dams and reservoirs, are the most challenging ones (Breeze, 2018). To find the optimal site for the construction of a hydropower plant is extremely challenging because displacement of people and wildlife and destruction of ecologies should be avoided.

Breeze (2018) states that careless and reckless development of hydropower damaged its reputation in the second half of the 20th century. Since then, rules and restrictions have been updated and modernised, which has led to a more ecological development process of hydropower projects. Well-designed and carefully executed hydro projects are one of the core elements of an environmentally friendly future, since investments in renewable sources of energy enable the possibility to move more and more away from the usage of short-term fossil fuels. The power generated from hydropower plants also allows the establishment of new industries.

Hydropower plants are classified mainly due to the height of the water head, or the amount of power generated to the grid. When comparing head heights, water heads less than 50 m are classified as low, water heads between 50 and 205 m as medium, and high if they exceed 250 m. Regarding power generation capacities, 100 MW and more classifies as a large hydropower plant, 15-100 MW as medium, 1-15 MW as small, 0.1-1 MW as mini, and power plants with a capacity below 0.1 MW are classified as micro power plants (Ahmad, 2018).

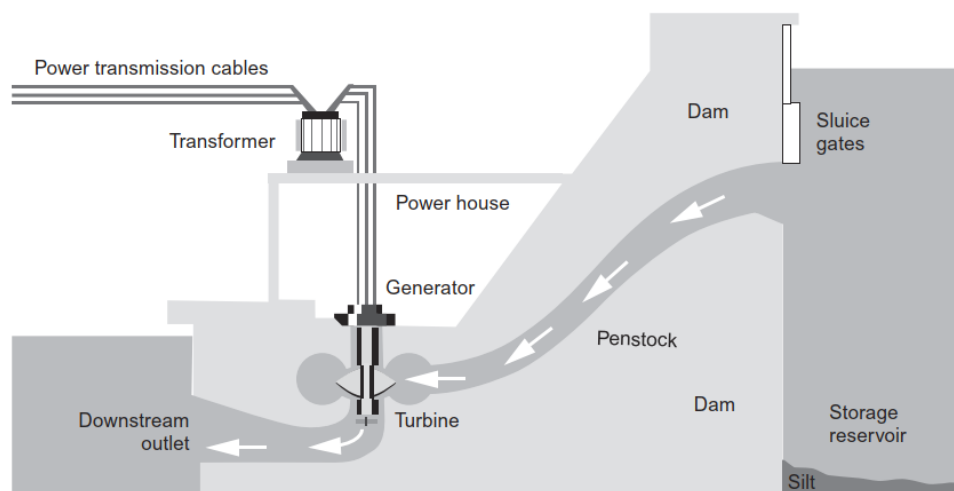


Figure 1. Hydropower plant with dam and reservoir (Breeze, 2019).

According to Breeze, hydropower often appears to be an expensive investment, but long-term it can become one of the cheapest sources of energy available, if accounted correctly. In the past 20 years, wind and solar power have grown

significantly. Since these sources of energy are so weather dependent, hydropower has been recognized as an optimal tool to balance the power generation to the grid from the renewables.

Pumped storage hydropower plants are excellent to increase the flexibility of power generation from hydropower plants even further (Breeze, 2018). The main idea is to pump water upstream to the reservoir and release it through the turbine when needed. The pumping usually occurs when the electricity prices are the lowest and the releasing when the prices are the highest, or when the demand for electricity is high. In other words, hydropower generation is very easily regulated and is therefore an optimal tool for maintenance of the balance in the grid.

Power converted to electricity is calculated by equation (1), according to Ahmad (2018):

$$P = \eta \cdot \rho \cdot g \cdot Q \cdot H \quad (2-1)$$

where P is the power output (W),  $\eta$  is the dimensionless efficiency of the turbine,  $\rho$  is the density of water ( $\text{kg/m}^3$ ), g is the gravitational acceleration ( $\text{m/s}^2$ ), Q is the volumetric flow rate, and H is the height of the water head (m).

### 2.1.1 Hydropower statistics

Breeze states that hydropower is the most impactful source of renewable energy, since it has supplied a huge part of the consumed electrical power in the world. According to statistics, hydropower has contributed to 15.4% to 20.3% of the annual electricity generation in the world between 1970 and 2015 (Breeze, 2018). Exact annual numbers are difficult to define, since the hydropower generation is highly dependable of the global rainfall. The total amount generated has increased annually in the past 60 years, but the power percentage generated by hydropower has slightly decreased, due to technical developments in the other fields of renewable energy sources as well. Even though most of the countries today have hydropower generation capacity, only a small number of large producers dominate the global

generation. China is by far the largest hydropower producer in the world with a generation of 1130 TWh in 2015, which was equal to 28.4% of the total generation the same year, according to Breeze.

In its report from 2020, the IEA states that in 2019, global net additions of hydropower reached only 12.7 GW. This was 45% lower than in 2018 and the lowest recorded since 2001. The decrease in growth is explained by China’s continued slowdown in the past few years. The statistics are affected strongly by this, since China is the global leader of net growth in the field of hydropower ever since 1996 (IEA, 2020).

The IEA forecasts the hydropower generation to expand 3% per year until 2030, which means that additions of capacity need to accelerate to return to the record level of 2013 by 2030 (IEA, 2020). Instead, capacity expansion has decreased. The statistics regarding global annual power generation with hydropower are presented in Figure 2. A steady increase has occurred during the past 20 years, but the annual net growth must increase to meet the forecasted values of 5 012 TWh by 2025 and 5 722 TWh by 2030 for the total annual generation. The trend downwards is expected to continue, mainly because the large producers China and Brazil do not have any ongoing large-project development now. This is due to restrictions and resistance towards projects from social and environmental aspects.

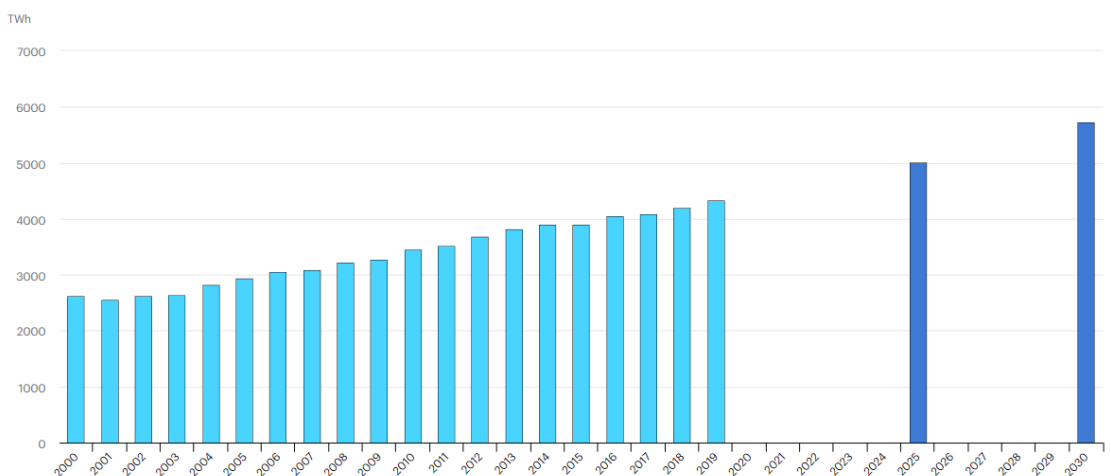


Figure 2. Global annual hydropower generation 2000-2030 (IEA, 2020).

The IEA (2020) estimates the hydropower generation to have increased by over 2% in 2019, due to continued recovery from drought in Latin America as well as large

capacity expansion and rich water availability in China. However, capacity additions overall have declined for the fifth consecutive year now. The few years to come are crucial for the capacity expansions, regarding the goals set by 2025 and 2030.

According to Tilastokeskus (2020), power generation from Finnish hydropower plants decreased by 7%, from 13.14 TWh to 12.24 TWh, between 2018 and 2019 due to low amounts of water. For the same reasons, the Finnish hydropower generation has decreased slightly for four years in a row already. However, the total share of renewables in Finland has increased during the past years, mainly due to increased usage of biomass and wind power. The corresponding value from 2018 to 2019 regarding biomass is an increase of 1% (104.10 TWh – 105.58 TWh). Wind power generation increased 3%, with an increase from 5.84 TWh in 2018 to 6.02 TWh in 2019.

### 2.1.2 Hydropower turbines

The main component in the machinery of a hydropower plant is its turbine. The turbine converts the mechanical energy forced by the flowing water into a rotational motion. The turbine is a relatively simple device regarding both its design and the materials used, which today are usually iron or steel. According to Breeze (2019), wooden turbines have also been used widely in the past. Modern turbines can achieve an efficiency up to 95%. This means that in the best-case scenario, only 5% of the energy contained of the water is lost, when the process is narrowed down to only concern the turbine. Figure 3 presents the designs of the most common turbines used in hydropower plants.



*Figure 3. The most common hydropower turbines. From left to right: Pelton,*

*Francis, and Kaplan* (Breeze, 2019; modified).

The Pelton turbine is the most common type of impulsive turbines. In these applications, the water is fed through a fine nozzle, which creates a high-speed jet of water. An impulse is formed when the jet hits the paddles of the turbine, which causes the turbine to turn. The Pelton turbine is used where the heads are the highest. A single Pelton turbine can operate with heads up to 1000 m and exceeding the limit means that the flow must be divided between several turbines. The preferred minimum value of the head is around 450 m, even though the theoretical minimum is around 200 m. The efficiency can be increased by adding up to four nozzles directed at the same turbine. Breeze states that the rotation speed of the turbine can easily be regulated by controlling the water flow through the nozzles. A reduction of the flow through the nozzles may often be preferred, since the Pelton turbine reaches its optimal efficiency when operating between 60% and 80% of the maximum load (Breeze, 2019).

The Francis turbine is a type of reaction turbine. A reaction turbine is a turbine that reacts to the potential energy above at the bottom of the head. Water is pressuring one side of the blades of the turbine, forcing it to react by creating a rotary motion. The Francis turbine is more suitable for heads below 450 m. The unique detail with the Francis turbine is the change of the direction of the water flow as it passes through the wheel (Breeze, 2019). The inflow of the water occurs radially towards the axis, but the interaction between the water and the blades forces the outflow to exit the turbine axially. Calculations are performed regarding the shape of the blades to maximize the mechanical energy extracted from the water flow. The parameters affecting the shape of the blades are flow volume and the height of the water head. With carefully designed blades, an efficiency of 90-95% can be achieved.

Where the height of the water head decreases to a level that Pelton and Francis turbines would not operate efficiently, the Kaplan turbine is often preferred. With a shape of a propeller, the Kaplan turbine is the number one choice for low water head applications, according to Breeze (2019). The typical height of a water head is around 10 m, and often even less. Power plants tend to install several Kaplan

turbines parallelly, since its efficiency drops dramatically when operated below 75% of the maximum load. During low water flows, some turbines may be completely shut down to allow the rest to operate within optimal efficiencies. Breeze states that this is an efficient way to maximize the total amount of power generated from the power plant. The key characteristics for the Kaplan turbine are its adjustable propeller blades. This enables flexible operation, which means that optimal efficiencies may be reached within a wide range of water flows, if the angles of the blades are calculated carefully.

According to Ismael Basael's book *Renewable Hydropower Technologies* from 2017, the design and innovation of turbines are the key factors to maintain a successful development in this field of technology. The blades of the turbine are the most vital components regarding the efficiency in the generation process from hydrokinetic energy. A turbine is subjected to different kinds of loads during its lifetime, such as inertial, gravitational and hydrodynamic forces. To achieve and maintain the optimal efficiency possible, the blades must be designed carefully. Optimal blade shape and design may also improve the lifespan of the turbine.

### 2.1.3 Pumped Hydroelectric Storage

According to (Francisco Díaz-González, et al., 2016), PHS systems are one of the most used forms of energy storage technologies. The main idea here is to store the water in the upper reservoir, by pumping it upstream from the lower reservoir when the demand and price of electricity is low, by utilizing power from the grid. When electricity demand is high, the water is released from the upper reservoir to the lower reservoir through a turbine. It is relatively simple to supply the peak demands of a power grid, since the operation of a hydropower plant can be started and stopped almost immediately (Bathia, 2014). The parameters affecting the amount of energy stored in the upper reservoir are the volume of the water stored and the height of the water head. The energy stored can therefore be calculated by:

$$E_{PHS} = \rho \cdot g \cdot H \cdot V, \quad (2-2)$$

where  $E_{PHS}$  is the energy stored (J),  $\rho$  is the density of water ( $\text{kg/m}^3$ ),  $g$  is the

gravitational acceleration ( $m/s^2$ ),  $H$  is the height of the water head (m), and  $V$  is the stored water volume ( $m^3$ ) (Francisco Díaz-González, et al., 2016).

Francisco Díaz-González, et al. (2016) state that the global hydro-storage potential could be up to 3000 GW. Figure 4 presents the operational principle of a pumped hydroelectric storage plant.

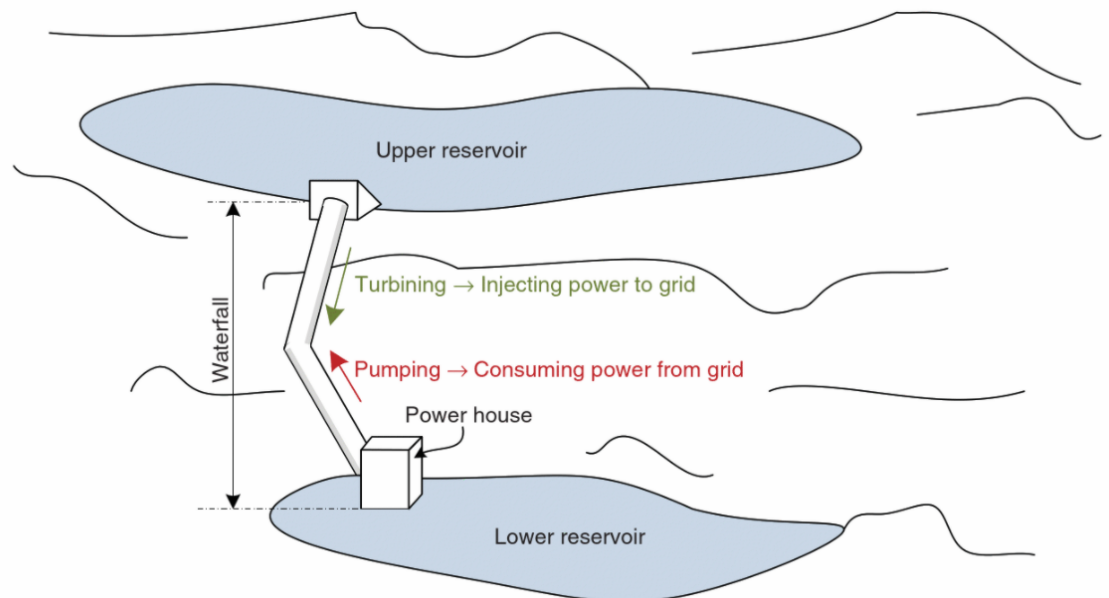


Figure 4. The operating principle of a PHS system (Francisco Díaz-González, et al., 2016).

Breeze (2018) states that new PHS systems are installed preferably to already existing dams, where the upper reservoir is already constructed. Depending on the location, it can sometimes be more convenient to construct both the reservoirs from scratch and not in a way of any waterways. A source of water must also be applied in this case, to initially fill the storage up. Water may also be lost over time from the system, which means that the system must be replenished (Breeze, 2018). Depending on the size of the storage and the number of turbines, the storage capacity can vary from usually 4 hours of power up to 20. The efficiency of the energy stored is estimated to be 70%-80%, if operated in a daily cycle.

#### 2.1.4 Dams

Schmutz & Sedzimir state in their book *Riverine Ecosystem Management* from 2018 that a dam is a barrier for obstruction of the waterflow and to construct a reservoir. These reservoirs are constructed to aid the specific needs for the community, such as electricity via a hydropower plant, water for drinking, cooling and industrial purposes, agriculture, regulation of waterflow and flood control, and recreation and fisheries.

Even though dams possess many positive qualities, they also have their drawbacks. Dams unfortunately damage the water life in the river basins and therefore force balance changes to the ecological system in the rivers. When a dam is constructed in a river, the ecosystem of the river at a reservoir comes to remind more of an ecosystem in a lake, due to radical changes in the waterflow (Schmutz & Sedzimir, 2018).

During construction of a dam, a spillway for the water is an important aspect to pay attention to. The spillway allows the water to flow through it if the flow in the river is higher than the intake capacity to the turbine (Schmutz & Sedzimir, 2018). These scenarios cause the water level to increase upstream from the dam and, therefore, spillways must be utilized to avoid water to flood over the dam. This should be avoided at any cost, since water flooding over the dam could eventually lead to its failure, followed by devastating consequences. Some dams, depending on size and location, must also be featured with ship locks to allow shipping to pass the dam, or passages for fish, especially on rivers where migratory fish spawn.

For different applications, different types of dams are preferred. Regarding both large and small hydropower plants, embankment dams, gravity dams, buttress dams and arch dams are used. Each of these has its own specific characteristics for different types of situations (Breeze, 2018).

Embankment dams are constructed from natural materials, which are mainly sourced locally nearby. Earth fill embankment dams and rock-filled embankment dams are

the two types of embankment dams. Their operating principles are very similar, the choice of material is often decided based on the local access. A core, usually of concrete or clay, is attached to the subsurface to prevent water to flow beneath it. Layers of rock or earth are then covering the core to create a sloping wall of the material used. The walls of material can be constructed on both sides of the dam, or only on the downstream side (Breeze, 2018). In that case, the upstream side is sealed with concrete. The spillway is especially important at embankment dams since the material may encounter erosion if the dam is overfilled. Embankment dams can be constructed on a wide variety of locations, since it does not impose large amounts of pressure on the foundation due to construction materials being relatively light. Embankment dams are usually well suited in valleys which are to be dammed (Breeze, 2018).

Gravity dams are another type of dam. Gravity dams are enormous dams, which are constructed from concrete or masonry, or a combination of these. The dam keeps its position due to gravitational forces applied on its mass. Gravity dams can be constructed a few hundred meters tall, with an almost vertical side upstream, while the downstream side has the shape of a slope. The dam applies enormous amounts of pressure to the foundations, due to its weight and size. Therefore, a foundation of secure rock is necessary in these kinds of applications. Gravity dams possess the characteristics to fit in both in wide and narrow valleys and can store large amounts of water upstream, since it is possible to construct the dams high due to its solid construction materials (Breeze, 2018).

Buttress dams are like concrete gravity dams, with the main difference that buttress dams are supported by triangular-shaped buttresses from the downstream side to aid the dam to resist the pressure generated from the water volumes on the upstream side (Breeze, 2018). The buttresses are massive walls constructed in the rock foundation downstream. Buttress dams require less construction material in comparison to the gravity dams, due to their design. Therefore, buttress dams are usually more economically beneficial.

Concrete arch dams are the fourth type of dam used at hydropower plants. Concrete

dams, like gravity dams, are large to their size and can store enormous capacities of water on the upstream side (Breeze, 2018). The physical characteristics of the parabolic structure of the dam allows redirection of the pressure along the line of the parabola. This means that all forces on the dam structure are resolved into compressive stresses due to tensile stresses being eliminated. Concrete arch dams have strict requirements on the surrounding environment, only steeply sided rock ravines fulfill the construction requirements for the dam. The rock of the valley walls supports the dam against the pressure caused by the water. Concrete arch dams are the strongest and most firm dams, due to the precisely engineered parabolic shape of the structure. The design also allows the dam to be relatively material efficient (Breeze, 2018).

#### 2.1.5 Economical aspects regarding hydropower

According to Breeze (2018), operation of a hydropower plant is a minor aspect to the entire investment cost, due to low overall maintenance costs. A major part of the budget for a hydropower plant is directed for the construction itself. The downside of this kind of project is that a major part of the funding needs to be available at the very beginning of the project. The funding of a construction project of a hydropower plant has shifted from being funded by the public sector to the stage where it is funded by private sector companies (Breeze, 2018). This is mainly due to the liberalization of electricity markets in the 1980's, when private sector companies started to acknowledge possibilities in the field of energy generation.

By turbine maintenance and component replacement in a hydropower plant, the operating lifespan may exceed even 100 years, which is 60-70 years longer than most other types of power plant. This is also an important aspect to pay attention to during calculation of project costs (Breeze, 2018).

The size of the power plant plays a huge part in the economics as well, since smaller power plants tend to have a higher relative capital cost than larger power plants, even though the construction cost of a larger power plants is higher (Breeze, 2018). Levelized cost of electricity (LCOE) is an economic model used to compare power

plants with the focus on the cost of the electricity generated. LCOE is a function which includes both capital and funding costs, as well as the operation and maintenance costs for a power plant. The equation should also include calculations of interests on loans and even decommission costs after the power plants service. This model allows comparison even between power plants that utilize different energy sources.

The LCOE calculations are performed at an early stage of a power plant construction project since that is the period where the results of the calculations are needed. Parameter estimations are required to perform the calculations, since the power plant does not yet exist, and therefore data of operation and maintenance is still unavailable. By using the discount rate, future costs are converted to equivalent values today, to achieve as realistic values as possible in the planning phase. Despite containing flaws and assumptions, the LCOE is model the most common today to calculate the generation costs of electricity at new power plants (Breeze, 2018).

### 2.1.6 Affects of climate change on hydropower

The future global climate changes are predicted to have its effects on hydropower generation in the decades to come. These changes vary regionally, since climate change does not impact every square meter of the planet equally (Hamududu & Killingtveit, 2012). Regarding existing hydropower systems, climate change will not have significant impact. However, future hydropower construction projects may be challenging by different grades, depending on the region. Electricity generation from renewable energy sources is predicted to triple from 2008 to 2035 (IEA, 2011), and since hydropower is a major part of power generation from renewables, this prediction can be challenging to meet if the acceleration rate of climate change would increase.

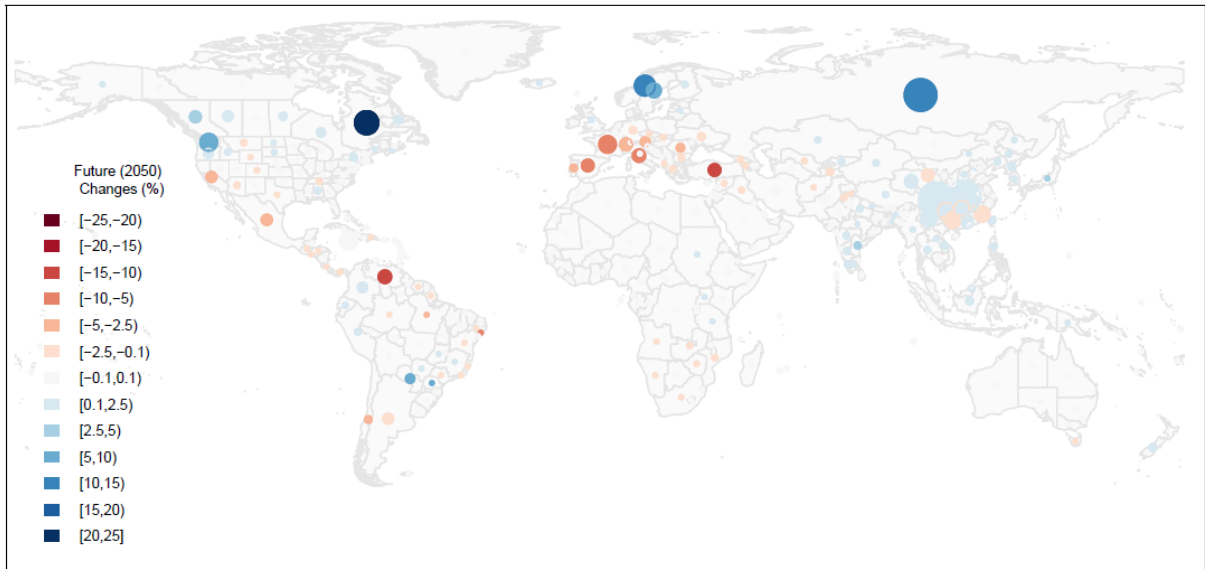


*Figure 5. Prediction of global hydropower generation changes by 2050 (Hamududu & Killingtveit, 2012).*

Continently, Asia is the continent with the most potential growth for hydropower, with a predicted increase of 0.27%. North and South America is the only other continents to have a positive margin in the potential growth, with 0.05% respective 0.03%. Australia is predicted not to have almost any changes, therefore a margin of 0% is predicted to occur in the continent (Hamududu & Killingtveit, 2012). Africa and Europe are the two continents to suffer from climate change regarding the power generation numbers. Africa is predicted to lose 0.05% and Europe 0.16% of their current hydropower capacities.

Even though a negative growth is predicted for Europe, Northern Europe is predicted to be the third most growing region percentagewise, after Eastern part of North America and Central Asia, according to Figure 5. Northern Europe will have an increase of 3.32 TWh of electricity generated, which is equal to a growth of 1.46%. Globally, the change will be a positive value of 0.08%, which is an increase of 2.46 TWh. Conclusions can be taken that as seen for now, climate change will not have significant impact on the field of hydropower (Hamududu & Killingtveit, 2012).

## 2.2 Generators

An electric generator is a device to convert mechanical energy into electricity. The generator consists of two main components, the stator and the rotor. The stator is the stationary part of the device, and the rotor is the rotary part. The turbine is attached to the rotor via an axis, and therefore forces it to rotate (Warne, 2005). The rotation may be further adjusted by installation of a gearbox between the turbine and the generator. The rotor is embedded by excitation windings, which are fed by a direct current to create a magnetic field inside the generator. The stator also contains windings (Warne, 2005). Mechanical energy is converted to electrical energy through electromagnetic induction in the generator. The voltage induced is created by the motion of the magnetic field and the conductor materials in the generator and is proportional to the rate of change in the magnetic flux (Thomas, 1972).

The voltage induced is calculated by Faraday's Law of Electromagnetic Induction:

$$\varepsilon = -N \frac{\Delta\Phi}{\Delta t} \quad (2-3)$$

where  $\varepsilon$  is the voltage induced in volts,  $N$  is the number of loops,  $\Delta\Phi$  is the change in the magnetic flux, and  $\Delta t$  is the change of time (Thomas, 1972).

The energy in the primary source is converted to electricity to certain voltages and frequencies via generation, transmission, and distribution, according to Figure 6. Boldea argues that larger systems tend to be more stable to operate.

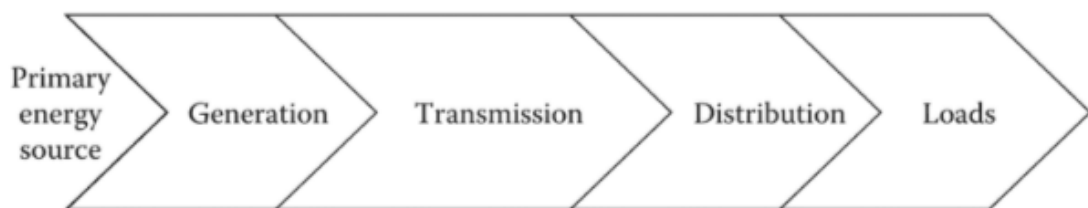


Figure 6. The standard value chain power grid (Boldea, 2016).

Synchronous, induction, and parametric generators are the three main types of generators. The synchronous generator is the type used at power plants and will therefore be the only type considered in the thesis.

### 2.2.1 Synchronous generators

Synchronous generators are characterized by a combination of a stator core including AC windings of one-, two-, or three-phase and a rotor which is DC excited or permanent magnet excited. The DC magnetic field generated in the rotor causes the stator frequency to depend on the rotary speed (Boldea, 2016). The generators in hydropower plants are usually a variant with a salient-pole concentrated excitation rotor with usually a high number of poles, as presented in Figure 7.

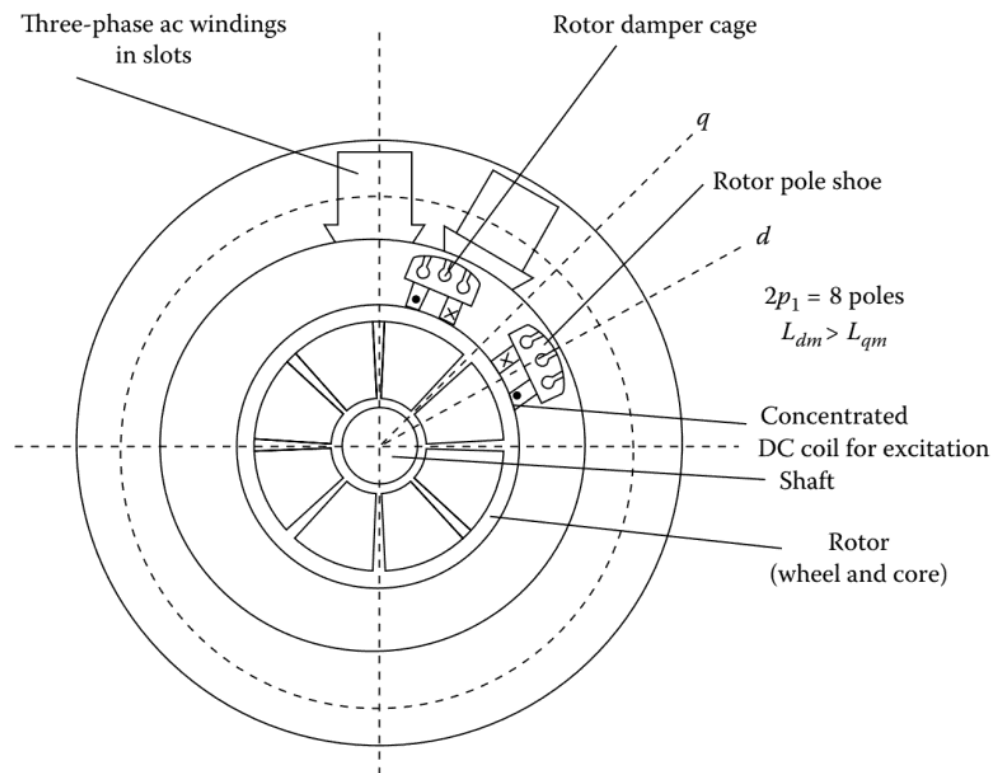


Figure 7. Synchronous generator with salient pole heteropolar DC-concentrated excitation (Boldea, 2016).

The rotor is constructed of solid iron to improve heat transmission and mechanical rigidity in the system. Generators in hydropower plants operate at a relatively low peripheral speed when compared to turbo generators. This means that a greater

number of poles are needed. The upper limit for the peripheral speed in a salient pole rotor is theoretically around 80 m/s (Boldea, 2016). However, the excitation coils must be protected against centrifugal forces caused by the rotation, even if the rotation speed is relatively low. Mild magnetic solid steel is the material of which the rotor poles are constructed, while laminations are used during the production of the rotor pole shoes. A generator's synchronous speed is given by equation 2-4:

$$N_s = \frac{120 \cdot f}{P} \quad (2-4)$$

where  $N_s$  is the synchronous speed in rpm,  $f$  is the frequency in Hz, and  $P$  is the number of poles.

When  $N_s$  is known, the generator's peripheral speed can be calculated according to equation 2-5:

$$N_p = \frac{\pi \cdot D_r \cdot N_s}{60} \quad (2-5)$$

where  $N_p$  is the generator's peripheral speed in m/s,  $\pi$  is a constant,  $D_r$  is the rotor diameter in m, and  $N_s$  is the synchronous speed in rpm. The peripheral speed is generally increased with increased power (Boldea, 2016).

The number of slots per pole is usually between 6 and 12, when the number of poles is high, while the number of slots per pole and phase is usually between 2 and 4. As previously mentioned, the rotor needs to be excited for the generation of the magnetic field. The power required is fed to the rotor windings by either copper sliprings and brushes, or by brushless excitation systems (Boldea, 2016). The DC excitation currents are controlled and regulated by a rectifier to maintain the required frequency stabilities and voltages. The rectifier has a voltage reserve of its own since the DC current is needed in the rotor windings as quickly as possible.

### **2.3 Generator protection functions**

This chapter will cover different faults that may occur on generators and its

surrounding equipment, and how to set protections against them.

The scale of protection equipment utilization varies from case to case. The potential risk of damage caused on generators, the size of the power plant and the consequences of interruptions of power generation are considerations which are evaluated when setting the requirements of the protection equipment on the generator. Over usage of protection equipment results in unnecessary expenses and increases the number of potential sources where faults may occur (Mörsky, 1992).

The specific protection functions covered in detail in the thesis are stator ground fault, stator overload, rotor ground fault, overcurrent, under-impedance, differential overcurrent, current unbalance, under-excitation, over-excitation, undervoltage, overvoltage, frequency, reverse power, shaft current and out-of-step protection.

To calculations of the protection settings for the certain functions are based on the following parameters:

*Table 1. Generator parameters.*

<i>Parameter</i>	<i>Symbol</i>	<i>Unit</i>
Rated output	S	MVA
Rated voltage	U	V
Rated frequency	f	Hz
Direct axis sub-transient reactance	$X_d''$	%
Direct axis transient reactance	$X_d'$	%
Direct axis synchronous reactance	$X_d$	%

These parameters are given by the manufacturers. The ratios of current and voltage transformers are additional data that needs to be known beforehand.

The following calculations can now be executed with the data from Table 1:

- Generator active power,  $P_{GN}$  (MW), by formula 3-1:

$$P_{GN} = S_{GN} \cdot \cos\phi \quad (2-6)$$

- Generator reactive power,  $Q_{GN}$  (MVar), by formula 3-2:

$$Q_{GN} = S_{GN} \cdot \sqrt{1 - \cos^2\phi} \quad (2-7)$$

- Generator nominal current,  $I_{GN}$  (A), by formula 3-3:

$$I_{GN} = \frac{S_{GN}}{U_{GN} \cdot \sqrt{3}} \quad (2-8)$$

- Generator nominal secondary current,  $I_{GN2}$ , by formula 3-5:

$$I_{GN2} = I_{GN} \frac{I_{CT2}}{I_{CT1}} \quad (2-9)$$

- Generator impedance,  $Z_{GN}$  ( $\Omega$ ), by formula 3-4:

$$Z_{GN} = \frac{U_{GN}^2}{S_{GN}} \quad (2-10)$$

### 2.3.1 Stator ground fault

The type of ground fault protection required depends on the grounding method used for the generator, and the values of ground fault currents. The values of the current between phase and ground can range from currents almost equal to zero, and up to three-phase fault currents. When the stator ground fault current transfers from the stator terminals towards the neutral, it decreases linearly. Generators are less protected against ground faults when the available ground fault currents are low, as shown in Figure 8. This means that a huge part of the winding could remain unprotected, if the value of the ground fault current would be below the rated load current for the machine.

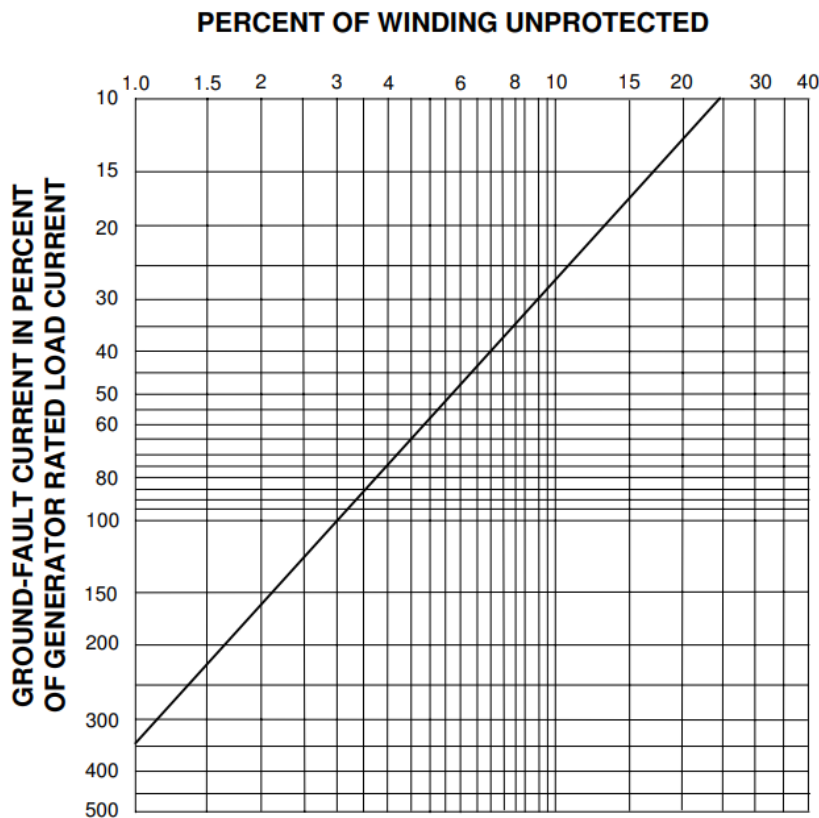


Figure 8. The relationship between unprotected winding (%) and available ground fault current (% of rated load current) (IEEE, 2007).

High-impedance grounding is a type of grounding used for generators and which can be divided in two sections, high-resistance grounding, and ground fault neutralizer

grounding. When a generator is grounded by these methods, separate backup protection is often needed, since phase-to-ground faults cannot be detected by differential relays in these cases. The reason is that the high values resistance and reactance in these systems limits the currents down to undetectable levels for the differential relays. A time-delay overvoltage relay is usually used in these applications since they are sensitive to detect voltages for the essential frequencies. When phase-to-ground faults occur, the voltage from phase to neutral will transfer through the grounding device, since the grounding impedance is a huge value in comparison to other impedances in the system. This scheme usually detects faults to within 2%-5% of the stator neutral, if the overvoltage relay is set to pick up minimum voltages of near to 5 V. The 64S scheme offers a 100% protection against stator ground faults. In this scheme, a subharmonic voltage (usually 15-20 Hz) is fed through shunt capacitances in the stator windings to ground, at normal operational conditions. The level of the measured current increases when a stator ground fault occurs, since it causes the shunt capacitances to short-circuit, which enables the relay to detect the fault (IEEE, 2007).

Low-resistance grounding is often utilized at systems where several generators are connected to the grid through a step-up transformer. This grounding method can be protected by two different protection methods, a time-overcurrent relay, or by a current-polarized directional relay. The time-overcurrent relay is set to be sensitive to detect currents above the limits set, and the delay is set to 25 cycles or more. In the scheme including the current-polarized directional relay, the operational coil detects differences in currents between the phase CTs remaining current and current in the neutral CT. In both cases, time-coordination of the mentioned relays with the remaining relays in the system is unnecessary, since only faults covered by the differential is detected, due to these sensitive methods (IEEE, 2007).

Reactance grounding is the third type of grounding for generators. This method is used at generators connected to distribution systems, which already have effective grounding. Differential relays can protect the stator phase windings almost completely against ground faults, due to the ground fault current levels available are 25%-100% of the three-phase fault current. In some cases, other sensitive ground

fault protection may be required since it may be challenging for differential relays to detect high-resistance faults. Reactance grounding is usually performed by a grounded wye-delta transformer, or a zigzag transformer (IEEE, 2007).

The 95% protection scheme is often used at hydropower plants. The process is more simplified, since protection of only 90-95% of the stator windings allows detection of ground faults by measuring the zero-sequence voltage either at the generator null point, or at the VT broken delta. The advantage here is that no injection device is needed.

The voltage which represents a 100% ground fault can be calculated to the secondary side:

$$U_0 = U_{GN} \cdot VT_{RATIO} \quad (2-11)$$

where  $U_0$  is the 100% ground fault voltage in the secondary (V),  $U_{GN}$  is generator nominal voltage (V), and  $VT_{RATIO}$  is the ratio of the voltage transformer.

The voltage setting is calculated as:

$$U_{0,setting} = U_0 \cdot 0.05 \quad (2-12)$$

### 2.3.2 Thermal overload

Generator overload, cooling system failure, core lamination insulating failure, and winding failure are faults that may damage the stator. Generators operate at a specific voltage, frequency, and power factor to fulfill cooperation requirements set by the power grid. The unit for a generator's capability output is kVA (kilovolt-ampere). The capability output, voltage, frequency, and power factor may differ by 5% from the rated values for the generator to still be able to operate. According to IEEE standards, the output capability may be exceeded shortly at emergency situations as presented in Figure 9. The exact numbers for the armature current are 115% for 120 seconds, 127% for 60 seconds, 150% for 30 seconds, and 218% for 10 seconds (IEEE, 2007).

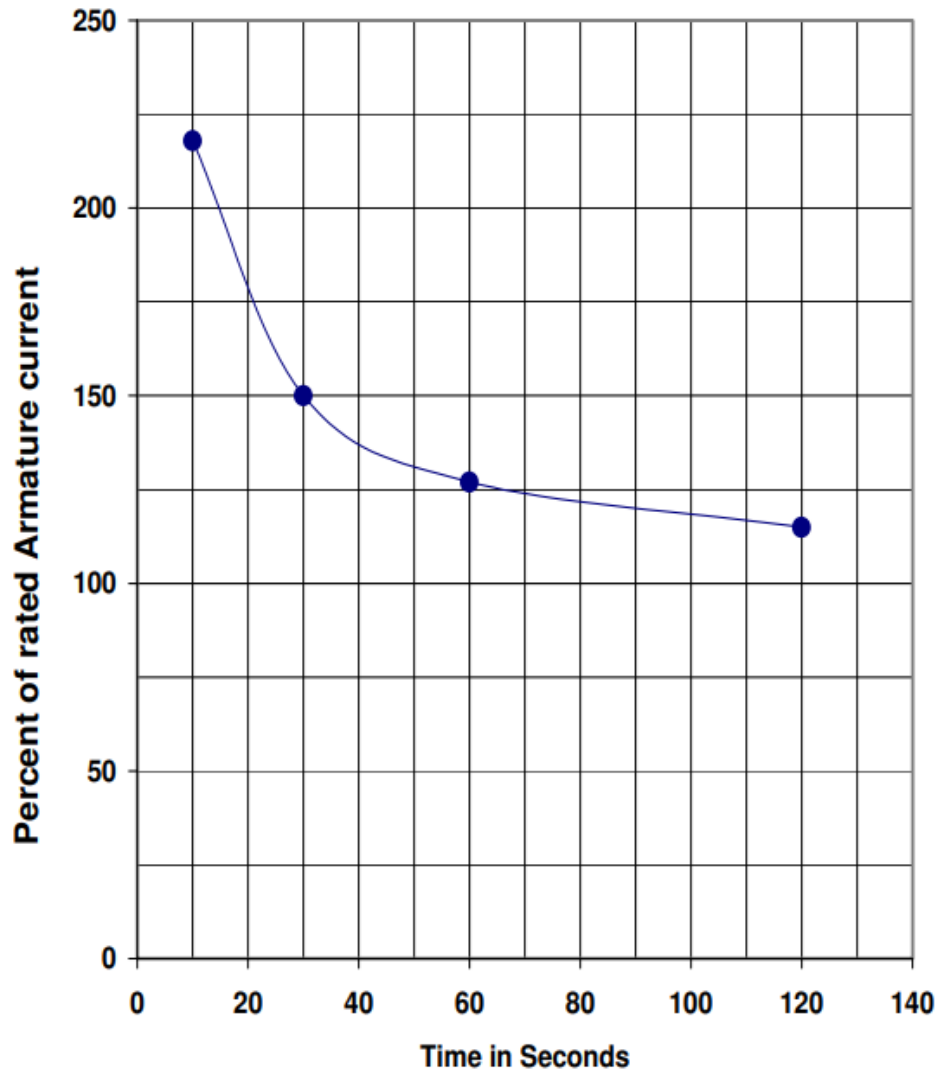


Figure 9. A generators short time thermal capability (IEEE, 2007).

Resistance temperature detectors and thermocouples are used to monitor the stator windings. The RTD tracks the resistance variations in the sensor to convert the data into a value of temperature, while the TC tracks the thermo-electric voltage variations induced in the sensor to obtain a temperature. The temperature data is connected to a relay for purposes to record, initiate corrective actions, trip, or to set off an alarm while continuously monitoring the stator windings. RTDs can also obtain the temperature data while installed between the top and bottom bars when the generator has indirect cooling on the stator windings. Where to stator winding cooling is direct, temperature values of the stator bar coolant discharge are obtained, alongside the data from the embedded RTD (IEEE, 2007).

Generators are also protected against failure of the cooling systems. Cooling systems are divided in two main parts, direct cooling, where the coolant is in direct contact with the high-temperature parts of the stator winding, and indirect cooling, where the cooling system works more like a heat exchanger where heat is transferred away from the generator through its insulation. The insulation of the stator core lamination or the winding conductors are at great risk to suffer serious damage if the cooling system would fail. To monitor and to keep track of temperatures in the windings and coolants, RTD's and TC's are used. Sensors are also used to track the flow and pressure of the coolant, for which somewhat different sensors may be used. Flow and pressure measurements are important to detect leakages as quickly as possible (IEEE, 2007).

Sometimes, overheating in the stator core can be caused by lamination insulation failure, even though the cooling system would operate as intended. The possible risks leading to lamination insulation failure are mainly vibration, damage to the core, or other parts of the machine are forced from their normal position due to various reasons. Lamination insulation failure can also lead to eddy currents, which result in further heating of the stator by creating contacts between the laminations. This leads to short circuits between the laminations, which results in the core steel to melt (IEEE, 2007).

The generator field is also at risk of receiving damage due to overheating and must therefore be protected. To produce the kVA within the required voltages and power factors, the field winding must operate at the required current levels. The generator output is regulated to maintain the field current within the limits if the power factor is below the rated value. The value of the field current can exceed for a short period of time. The exact numbers are 113% for 120 seconds, 125% for 60 seconds, 146% for 30 seconds, and 209% for 10 seconds. The allowed exceeded percentages for the field current are slightly below when compared to the limits for the armature current. The short time thermal capability for the generator field is presented in Figure 10 (IEEE, 2007).

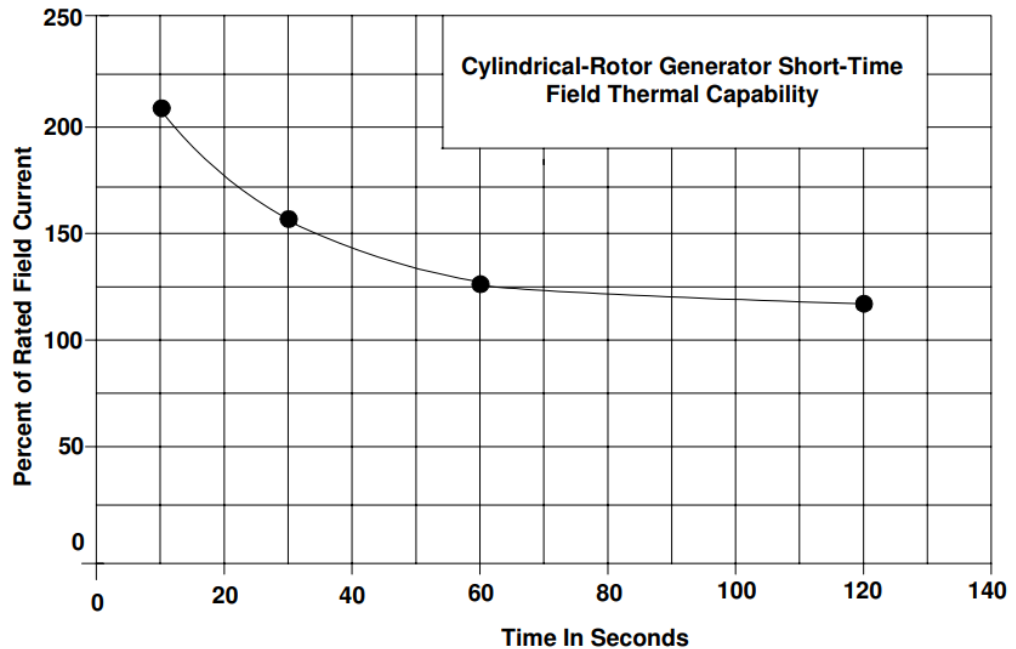


Figure 10. Generator field short time thermal capability (IEEE, 2007).

Usually, the temperature in the field windings is monitored indirectly since it is relatively challenging to install temperature sensors directly in the field winding. In some systems, the average temperature of the field windings can be tracked by calculating the field resistance by the field voltage and current. The calculated value is then compared to the resistance when the system is cold, and therefore, the field winding temperature can be approximated. The downside of this method is that when the average temperature is only approximated, the actual hot spots cannot be tracked (IEEE, 2007).

The inverse time-delay relaying scheme can be connected to the main generator field, the AC exciter terminals, or to the AC excitatory field. This method uses a voltage relay which should match the characteristics presented in Figure 10. This scheme is an alternative to remain the machine online even after system faults. The operation steps for the inverse time-delay relaying scheme are the as for the fixed time-delay relaying scheme (IEEE, 2007).

Some excitation systems may include both field protection and voltage regulation. This system reduces the field current to the full-load value or a preset value below the full-load. The system trips the regulator to switch to another exciter, and if

overexcitation still occurs, the generator is tripped (IEEE, 2007).

As for the rotor itself, indirect thermal measurement is preferred over direct thermal control and protection. However, methods to eliminate reasons for increased rotor temperature can be used. The reasons for increased rotor temperature are circulated currents in the rotor body, which are again caused by loss of excitation, loss of synchronism or negative-sequence currents in the stator (IEEE, 2007).

Following calculations are the steps included in this thermal model:

Preload current:

$$I_P = \sqrt{\theta} \cdot k \cdot I_{GN} \quad (2-13)$$

where  $I_P$  is the preload current (A),  $\theta$  is the temperature rise (for example, if the temperature rise is 110 %,  $\theta$  is expressed as 1.1),  $k$  is the overload factor and  $I_{GN}$  is generator nominal current. Overload factor is given by generator manufacturer.

Value for trip:

$$a = k \cdot k_\theta \cdot I_{GN} \quad (2-14)$$

where  $a$  is the value for trip,  $k$  is the overload factor,  $k_\theta$  is the ambient temperature factor and  $I_{GN}$  is the generator nominal current.

Trip time:

$$t = \tau \cdot \ln \frac{I^2 - I_P^2}{I^2 - a^2} \quad (2-15)$$

where  $t$  is the trip time (s),  $\tau$  is the thermal time constant (s),  $I$  is the measured rms phase current (A),  $I_P$  is the preload current (A), and  $a$  is the value for trip (Schneider Electric, 2018). These calculations are performed according to a thermal model from IEC 60255-8.

### 2.3.3 Rotor ground fault

The main concern regarding protection of the generator field includes detection of ground faults in the circuits. However, the operation of the machine will not be disturbed by a single ground fault since the field circuit is ungrounded. Unbalanced air gap fluxes will however occur during several ground faults, which leads to a short-circuit in a section of the field winding. This can launch a series of events, vibrations in the rotor may occur due to the unbalanced air gap flux, or unbalanced current in the windings, which again leads to increased temperatures. A short period of these faults may result in the machine to suffer serious damage. Therefore, several methods have been developed to protect the rotor field and its windings by detection of the ground faults as quickly as possible. The most common methods utilized are field ground detection with a DC source, a voltage divider, pilot brushes, or a low-frequency square-wave voltage injection (IEEE, 2007).

In the first type, the DC voltage source and an overvoltage relay are connected in series between the negative side of the field winding and ground. This setup enables the overvoltage relay to detect ground faults wherever in the field. To ensure the operation of the relay during ground faults, the rotor shaft may be grounded by a grounding brush. The reason is that the oil film in the bearing may cause the resistance levels to be of such level that it would create challenges for the overcurrent relay to detect the fault. According to IEEE (2007) standards, the time delay for the relay is to be set to 1-3 s.

When using the method that includes a voltage divider, an overvoltage relay is installed between the center point of the voltage divider and ground. A varistor is used to eliminate the problem of undetected faults that occur in the null point. Without the varistor, which is a nonlinear resistor, some ground faults in the field would remain undetected. The varistor is connected in series with one of the resistors, which are included in the voltage divider. It is often preferred that the null point would be at the center point of the field winding. This means that the divider is set to maintain the location of the null point at the center of the winding, when operating within the rated excitation voltages (IEEE, 2007).

In some cases, pilot brushes are applied to brushless systems, to gain access to the rotary parts of the field. This is a somewhat rare approach to the problem, since one advantage of brushless machines is to get rid of the brushes. Therefore, adding pilot brushes is unusually the most attractive method in most cases. Where rotator shafts are equipped with a collector ring, ground fault detection can be utilized by dropping a pilot brush within a time sequency to track the process (IEEE, 2007).

The operation principal of field ground detection with low-frequency square-wave voltage injection is that a square-wave signal of approximately +15 V is fed to the field. The strength of the return signal is then measured and compared to the injected value, to approximate the resistance in the insulation. Depending on the capacitance in the filed winding, the injection frequency is adjusted usually between 0.1 and 1 Hz. Based on the data obtained, ground faults in the field windings can be detected. Additionally, protection equipment tracking vibrations are often provided to this kind of protection (IEEE, 2007)

The leaking current between the rotor shaft and the rotor is calculated:

$$I_{leak} = \frac{U_{inj}}{Z_{fault} + Z_{coupling}} \quad (2-16)$$

where  $U_{inj}$  is the injection voltage (V),  $Z_{fault}$  is the impedance during earth fault ( $\Omega$ ), and  $Z_{coupling}$  is the injection device internal impedance ( $\Omega$ ).

According to ABB's REK 510 injection device user's manual,  $I_{leak}$  could reach over 100 mA, even up to 130 mA, during fully developed earth faults. The magnitude of the current is though dependable on the injection voltage, as presented in Equation 2-16.  $I_{leak}$  is usually no more than a few milliamperes during normal conditions.

In terms of insulation resistance, ABB recommends an alarm setting at minor earth faults for currents that correspond to an insulation resistance of no less than 10 k $\Omega$  with a 10 second time delay. The trip setting is set to pick up a current correspondingly to an insulation resistance of 1-2 k $\Omega$  with a time delay of 0.5 seconds (ABB Oy, 2007).

These recommendations only apply for the ABB REK 510, variations in settings recommendations might occur between different manufacturers and device models, and between different applications and system voltages.

Bender GmbH & Co. KG states that their insulation resistance monitoring device disconnects the unit from the load when the insulation resistance decreases below the value of 100  $\Omega$  times the system voltage (Bender GmbH & Co. KG, n.d.). When this value is reached, the insulation has been seriously weakened.

### 2.3.4 Overcurrent

Overcurrent relays may be used to track generator overloads. This relay consists of two main units, the first is the instantaneous overcurrent unit, which picks up at a current of 115% of the full load, and to control the second unit, the time-overcurrent unit. The time-overcurrent unit is usually set to pick up at 75-100% of the full-load current, while the time setting for the relay operating time is set at 7 s at 218% of the full-load current. This setup allows the relay to avoid any trips below 115% of the full-load current and to still provide trip at currents above 115% of full-load at the time set. Air-cooled generators may be relatively problematic to protect from capability overloads if the ambient temperature is high, since the ambient temperature plays a major part in air-cooled systems (IEEE, 2007).

The first stage of overcurrent protection is often set to detect overload currents of 10-30% of the generator nominal current. The trip time is determined by the IEC characteristics chosen. For example, the IEC Normal inverse characteristics could be a favorable option for the first stage protection.

Trip time for the different inverse characteristics is calculated by the equation below:

$$t = \frac{k \cdot A}{\left(\frac{I}{I_{pick-up}}\right)^B - 1} \quad (2-17)$$

where t is trip time (s), k is time multiplier setting, I is the measured current (A),  $I_{pick-up}$  is the preset pick-up value for current in relation to the generator nominal current

(A) and A and B is parameter constants. Constants A and B are determined from Table 2.

For example, by setting a stage 1 protection with 120% overload ( $I/I_{pick-up}$ ), and the time multiplier setting (k) to 0.2, the trip times for the different characteristics equals (from Equation 2-17 and Table 2):

Normal inverse (NI): 7.66 s

Extremely inverse (EI): 36,36 s

Very inverse (VI): 13.5 s

Long time inverse (LTI): 120 s

Table 2. Inverse delays constants according to IEC standards. (Schneider Electric, 2018)

Delay type		Parameter	
		A	B
NI	Normal inverse	0.14	0.02
EI	Extremely inverse	80	2
VI	Very inverse	13.5	1
LTI	Long time inverse	120	1

The second stage overcurrent protection is the protection against sudden faults, which often leads to high peak currents. The current setting is usually set just below the minimum generator short circuit current since the unit must trip at any sized short circuits in order to minimize damage to the generator and its surrounding equipment. The steady state 2-phase short circuit fault is the condition where short circuit current is the lowest and must therefore be used to determine the protection setting.

The minimum short circuit current can now be calculated:

$$I_{SC2} = \frac{U_{LL}}{2 \cdot X_d} \quad (2-18)$$

where  $I_{SC2}$  is the minimum 2-phase short circuit current (kA),  $U_{LL}$  is generator phase-to-phase voltage (V), and  $X_d$  is generator synchronous direct reactance ( $\Omega$ ). The

second stage overcurrent setting can now be set according to short circuit calculations above (Schneider Electric, 2005). The resistance during short circuits is so minimal that it can be neglected here.

Voltage dependent overcurrent:

$$I_V = \frac{I_{pick-up} \cdot S_{GN}}{U_{GN} \cdot \sqrt{3}} \quad (2-19)$$

current in relation to the generator nominal current (A),  $S_{GN}$  is generator nominal apparent power (VA) and  $U_{GN}$  is generator nominal voltage (V).

### 2.3.5 Under-impedance

The purpose of impedance protection is to detect faults by measuring impedance in the generator and comparing it to the nominal value. The impedance is calculated from the measured current and voltage at the generator null point side. Faults are recognized by lowered values in the measurement values. The impedance protection scheme works as a back-up protection for the differential protection schemes and should therefore be set accordingly to ensure selectivity in the protection coordination.

Impedance protection zones are set with different pick-up values and trip times, to enable selectivity in the protection. For example, Zone 1 could be set to cover the generator, Zone 2 to cover the distance between the generator and the low voltage side windings in the unit transformer, and Zone 3 could cover the grid. Since the focus is here on generator protection, Zone 3 will not be covered in the thesis.

Regarding Zone 1, impedance is only calculated for the generator according to equation X:

$$Z_{Z1} = \frac{U_{GN}^2}{S_{GN}} \quad (2-20)$$

where  $Z_{z1}$  is the zone 1 impedance ( $\Omega$ ),  $U_{GN}$  is generator nominal voltage (V), and

$S_{GN}$  is generator nominal apparent power (VA).

The zone 2 protection consists of the line impedance between the generator and the unit transformer plus the transformer impedance. The transformer reactance is calculated as:

$$X_T = \frac{U_{TSC} \cdot U_{TLV}^2}{100\% \cdot S_{TN}} \quad (2-21)$$

where  $X_T$  is transformer reactance ( $\Omega$ ),  $U_{TSC}$  is transformer short circuit voltage (%),  $U_{TLV}$  is transformer low voltage side nominal voltage, and  $S_{TN}$  is transformer nominal apparent power (VA) (Siemens, 2020).

The reactance of the line between the generator and the unit transformer is calculated as follows:

$$X_L = l \cdot X' \cdot \left( \frac{U_{TLV}}{U_{HLV}} \right)^2 \quad (2-22)$$

where  $X_L$  is the line reactance ( $\Omega$ ),  $l$  is the line length (m),  $X'$  is the line reactance per unit length ( $\Omega/m$ ),  $U_{TLV}$  is transformer low voltage side nominal voltage, and  $U_{THV}$  is transformer high voltage side nominal voltage (Siemens, 2020).

When Zone 1 is the only zone included in the impedance protection, the generator nominal impedance can be set to the reference point. In cases where zone 2 is added to the scheme, the generator synchronous direct reactance ( $X_d$ ) must be used instead of the nominal impedance. This is because impedances and reactances cannot simply be added together. The  $X_d$  is a percentage of the generator nominal reactance and is provided by the generator manufacturer.

When including Zone 2 in the impedance protection scheme, the total reference reactance is calculated as follows:

$$X_{REF} = X_d + X_L + X_T \quad (2-24)$$

When protection the entire block, the  $X_T$  is the deciding factor regarding the pickup value. When the transformer tap changers change position, the fault impedance is affected. Therefore, the trip value should be set to 70-90% of the  $X_T$ . According to Siemens Siprotec 5 manual, setting the trip to 70% is the safest option (Siemens, 2020).

This gives the equation:

$$X_{TRIP} = X_{REF} - (X_T \cdot 0.7) \quad (2-25)$$

The trip delay should be set to a maximum of 100 ms to ensure selectivity (Siemens, 2020)

### 2.3.6 Differential overcurrent

To protect the stator windings from phase fault, high-speed differential relays are used. Depending on how the generator is grounded, the differential relay may detect three-phase faults, faults between two phases, faults between double-phase and ground, and faults between a single phase and ground. Since the difference in current is 0 A between inflow and outflow in a phase winding, turn-to-turn faults cannot be detected by differential relays. Therefore, separate protection against this type of fault is needed. Regarding high-impedance grounded generators, the fault current levels are usually too low to be detected by differential relays due to the high impedance levels, and therefore must separate ground fault protection be applied (IEEE, 2007).

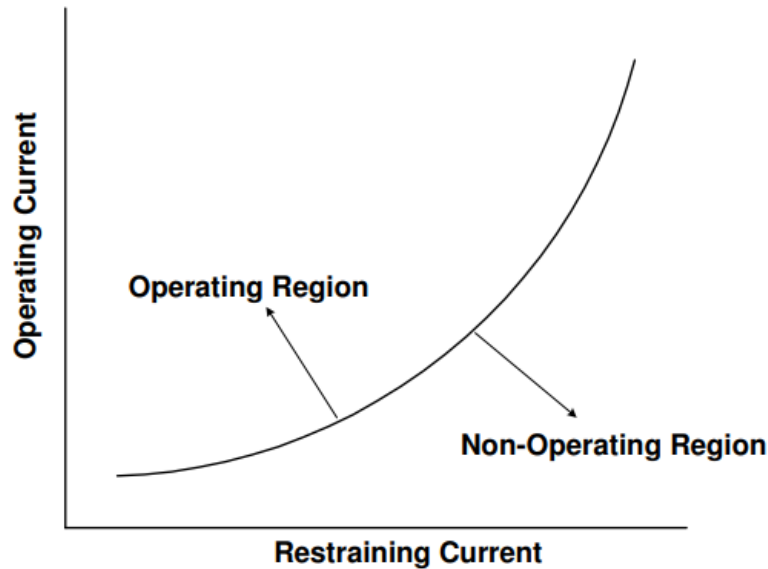


Figure 11. The slope differential relay (IEEE, 2007).

The variable slope percentage differential relay is the first type of three used for phase fault protection. The ranges of operation are presented in Figure 11. This type of relay is especially sensitive to detect internal faults due to the variation of the percentage slope characteristics. Depending on the values of through current, the percentage slope characteristics can range from 5% up to 50% (IEEE, 2007).

Another type of phase fault protection is the high-impedance differential relay. This type of relay can detect whether a fault is external or internal, by measuring voltage, since low voltages that passes the relay means external faults, while higher voltages mean internal faults. The high-impedance differential relays placement in the circuit is presented in Figure 12. This relay can detect fault currents for as low as 2% of the generators nominal current, while mainly focusing on three-phase or phase-to-phase faults in the stator windings. In comparison with the variable slope percentage differential relay, the high-impedance differential relay can detect operation disturbances more quickly, since this relay is more sensitive to faults, due to its design (IEEE, 2007).

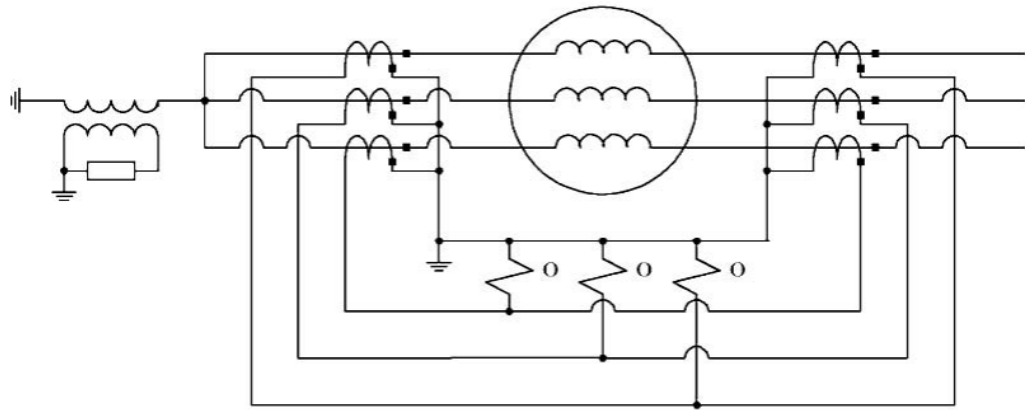


Figure 12. The high-impedance differential relay (IEEE, 2007).

The third main type of stator phase fault protection is the self-balancing differential scheme. This type of protection suits well for low-resistance neutral grounded generators. An instantaneous over current (IOC) relay detects incoming and outgoing currents in the winding, since both ends of a certain winding is connected to a current transformer's (CT's) openings, like presented in Figure 13.

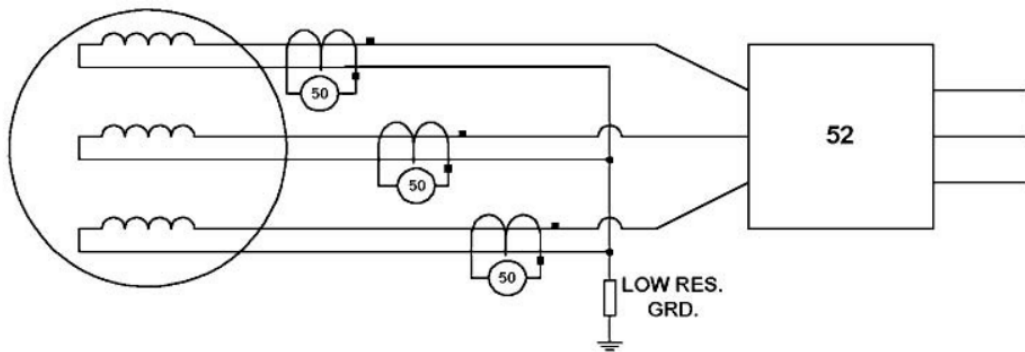


Figure 13. Self-balancing differential protection scheme (IEEE, 2007).

Figure 13 also illustrates that beyond phase faults, this scheme can also detect ground faults. The self-balancing differential protection scheme offers especially sensitive protection, since the CTs in the scheme can detect minimal current differences, due to its design. However, this design has its challenges in carrying continuous loads (IEEE, 2007).

Some generators also need turn fault protection if the stator is equipped with multi-turn coils. The stator winding circuits are divided in groups, in which currents are

compared by split-phase relaying to detect faults. However, hydroelectric turbines are usually equipped with single-turn stator windings. Therefore, this type of protection is unnecessary in those cases (IEEE, 2007).

Generators are also equipped with backup protection for the phase fault schemes. The type of protection required depends both on the size of the machine, and how it is connected to rest of the system. The overall differential scheme is the backup scheme that includes the generator, interconnections, and both the unit transformer and auxiliary transformer. Sometimes, protection of the auxiliary transformer may be inadequate, especially if the transformer is excluded from the overall scheme. The reason is that the differential relays gain no output current from the CT when faults occur on the auxiliary transformer's high side, since the currents can exceed the CT's rated current by over 100 times. This problem is avoided by utilizing the auxiliary transformer's low side as the connection point for the overall differential scheme. This means that the auxiliary transformer detects the minor faults, and the overall scheme detects the more severe ones (IEEE, 2007).

Bias current:

$$I_{BIAS} = \frac{|\bar{I}_1| + |\bar{I}_2|}{2} \quad (2-26)$$

Differential current:

$$I_{DIFF} = |\bar{I}_1 + \bar{I}_2| \quad (2-27)$$

where  $I_{DIFF}$  is the differential current (A),  $I_1$  is the primary winding current (A), and  $I_2$  is the secondary winding current (A).  $I_1$  and  $I_2$  can be found in Figure 14.

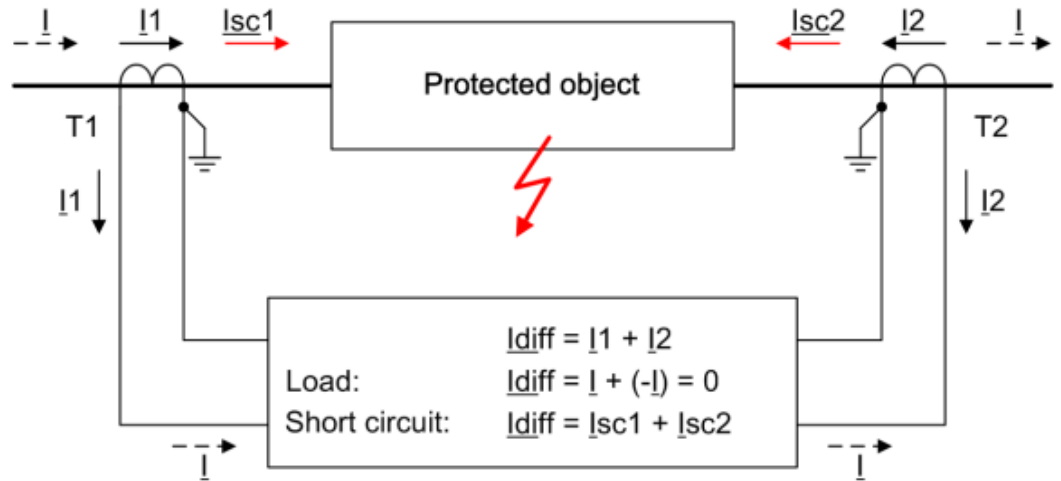


Figure 14. The differential protection scheme (Siemens, 2020).

To determine the minimum differential current in the generator, some margins are to be considered. These margins are the pickup accuracy of the relay, the expected CT mismatch during maximum permitted operational limits and a safety margin (usually 5%), The margin regarding relay pickup accuracy is provided in the relay manual (Le & Vu, 2019).

Setting (ABB REG670):

The differential relay characteristics for ABB REG670 is divided in 3 sections: Section 1, Section 2 and Section 3. Section 1 is aimed to be the pickup section, where the risk of encountering false differential currents is low. The purpose of Section 2 is to ensure detection of internal faults in the scheme at normal operating conditions, and Section 3 aims to increase the security major through-fault conditions (Le & Vu, 2019). The differential relay characteristics are presented in Figure X.

The pickup value is calculated from the following equation:

$$I_{d \min} = \frac{K_{REL} \cdot (2 \cdot K_{ERR,CT}) \cdot I_{GN}}{I_{CT}} \quad (2-28)$$

where  $I_{d \min}$  is the minimum differential overcurrent (%),  $K_{REL}$  is a reliable constant equal to 1.5,  $K_{ERR,CT}$  is the combined margin of expected CT mismatch and the safety margin (generally 5%),  $I_{GN}$  is generator nominal current (A), and  $I_{CT}$  is current transformer current (A).

Once obtained the  $I_{d \min}$ , the pickup setting can be determined, following the equation:

$$I_{d \min} < 87_{\text{setting}} \quad (2-29)$$

This means that the setting value needs to be greater than the calculated  $I_{d \min}$  to avoid unnecessary trips. Typical values here are 0.1, 0.15, 0.20, or 0.25 (Le & Vu, 2019).

The end points of section 1 and 2 can be calculated:

$$EndSection1 = \frac{0.5 \cdot I_{GN}}{I_{CT}} \quad (2-30)$$

$$EndSection2 = \frac{3 \cdot I_{GN}}{I_{CT}} \quad (2-31)$$

Recommended setting for SlopeSection2 is 30% and 80% for SlopeSection3 (Le & Vu, 2019).

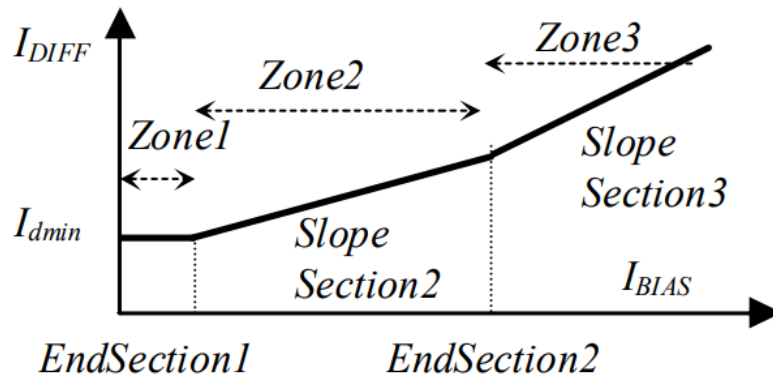


Figure 15. Differential slope characteristics for ABB REG670 relay (Le & Vu, 2019).

### 2.3.7 Current unbalance

Unbalanced loads and open phases are examples of faults, which may trigger unbalances in the three-phase current flows. The unbalanced current is known as the negative-sequence current,  $I_2$  according to IEC-standards, which can lead to serious

generator damage in a relatively short period of time. However, salient-pole generators should withstand  $I_2$  currents of the value of 10% continuously, if phase currents do not exceed 105% of the rated values, and if and the kVA-rating remains at the rated value, or below (IEEE, 2007). The capability to withstand  $I_2$  currents is expressed as  $I_2^2t$  and can be approximated according to Figure 16.

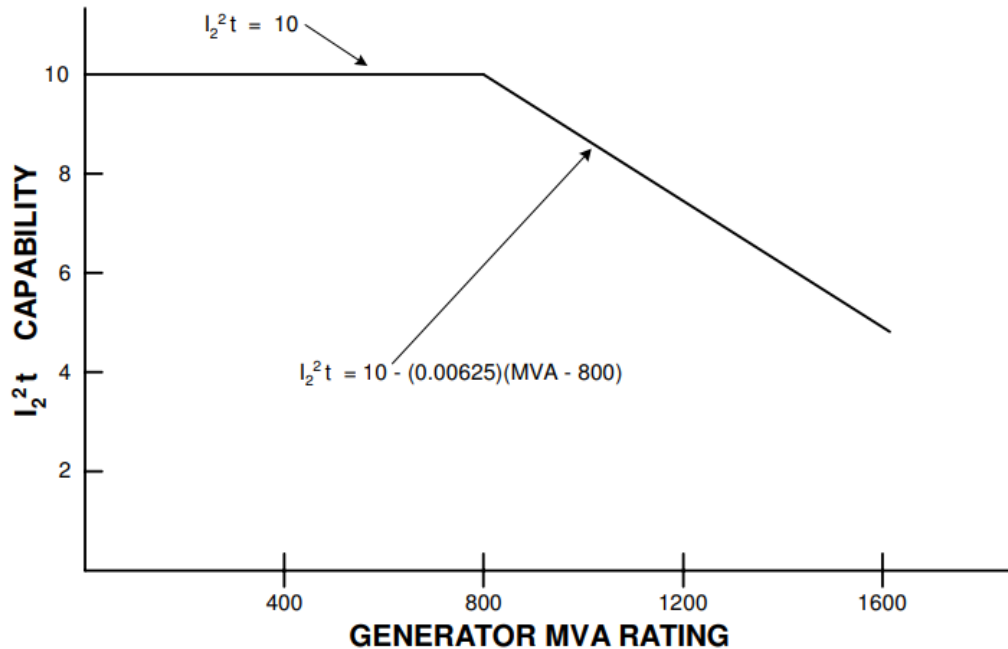


Figure 16. Generator capability of continuous  $I_2$  currents (IEEE, 2007).

Electromechanical relays or static/digital relays may be used for protection against unbalanced currents. In the electromechanical relays, the sensitivity is set to pick up unbalances in the current values of 0.6 pu (IEEE, 2007), which means per unit, and is used to express “the ratio of an actual or measured quantity to the base or reference value of the same quantity” (VELCO, 2013). This can also be expressed as variations of 60% of the rated values. The static or digital protection relays are more sensitive in comparison with the electromechanical relays, and can therefore detect minor faults, even unbalanced currents at the continuous capability operation. Some schemes are additionally equipped with especially sensitive protection alarm units, which may detect  $I_2$  currents from 0.03 pu to 0.2 pu. This can be used as a warning signal for exceeding the continuous capability of the generator (IEEE, 2007).

from IEC 60034-1, the continuous withstand is 8% of rating and the I<sup>2</sup> t value is 20s.

The reference current for the inverse delay characteristic is calculated as:

$$I_{REF} = \frac{\%I_2 \cdot I_{GN}}{I_{CT1}} \quad (2-32)$$

where I<sub>REF</sub> is the reference current (A), I<sub>2</sub> is the allowed current continuous unbalance (%), given from generator manufacturer) I<sub>GN</sub> is generator nominal current and I<sub>CT1</sub> is current transformer primary current.

Inverse delay

The time allowed to operate with unbalanced currents is calculated as:

$$t = \frac{K_1}{\left(\frac{I_{REF}}{I_{GN2}}\right)^2 - K_2^2} \quad (2-33)$$

where t is the allowed operation time (s), I<sub>GN2</sub> is the generator nominal secondary current (A), I<sub>REF</sub> is the reference current (A), K<sub>1</sub> is the delay multiplier (s) and K<sub>2</sub> is the pick-up setting. K<sub>1</sub> and K<sub>2</sub> are given by the generator manufacturer.

### 2.3.8 Under-excitation

Generator under-excitation may occur for several reasons, for instance due to open or short circuit of the field, field breaker failure, or failure in the excitation supply system or in the voltage regulator. Hydropower generators may operate within a load of approximately 20%-25% of the rated load and maintain the rated synchronism, even though a fault in the field occurs. This is due to the characteristics of the salient-pole rotor, with which hydropower generators are equipped, as previously mentioned. Faults that lead to under-excitation may eventually cause field and stator windings to suffer from damage. Distance relays are often used to detect the change of impedance from the generator terminals' point of view, and the loss of excitation can therefore be approximated (IEEE, 2007).

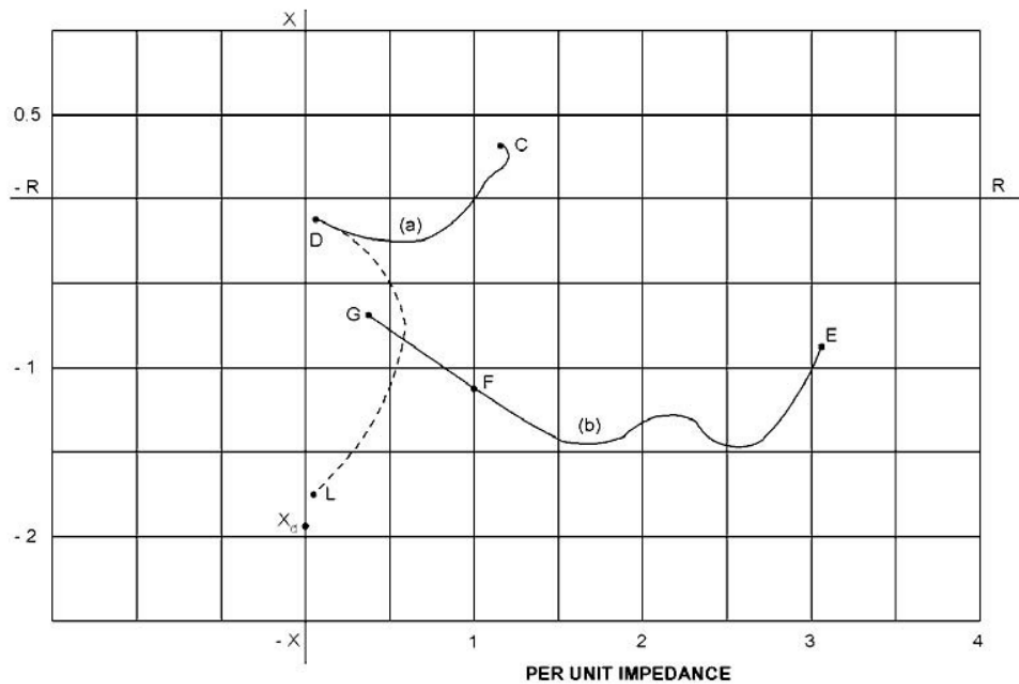


Figure 17. The characteristics for under-excitation (IEEE, 2007).

Figure 17 presents a comparison between the impedance variations of machine operating at full load, curve (a), and an under-excited machine operating at 30% of the full load, curve (b).

A capability curve presents the operational limits of a generator. The factors that apply strains to the operation are turbine power, rotor and stator limit, and the stability limit. Figure 18 presents the capability curve of a typical hydropower generator. A generator is underexcited when operating on the negative side on the X-axis (P), and overexcited when operating on the positive side. The capability curve is drafted only on the positive side of the Y-axis (Q) since generators do not operate with a negative value of active power.

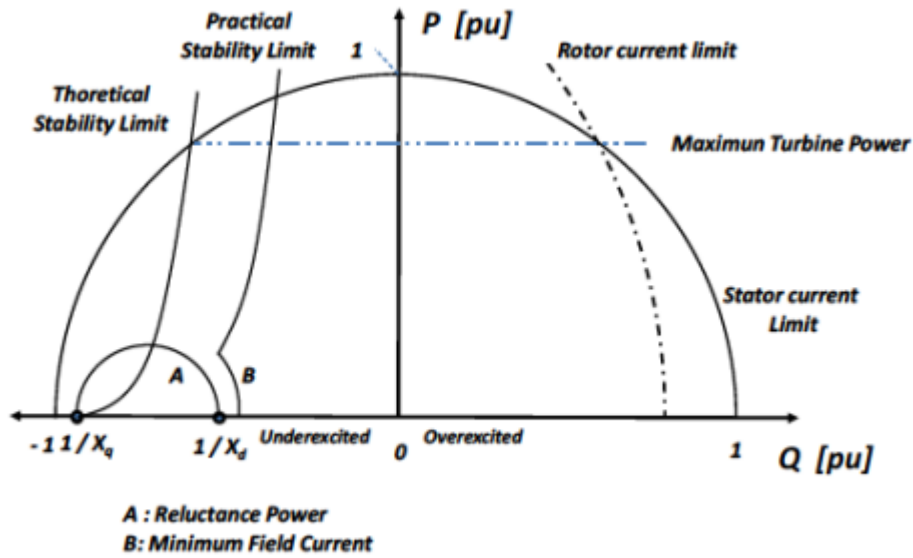


Figure 18. Capability curve of a typical salient pole synchronous generator (López, et al., 2017).

The loss of excitation area can also be expressed in a R-X plot, as presented in Figure 19. As mentioned above, the underexcitation zone is on the negative side on the reactive power axis. On the other hand, the loss of excitation trip zone is on the negative side of the reactance axis, but on the positive side of the resistance axis.

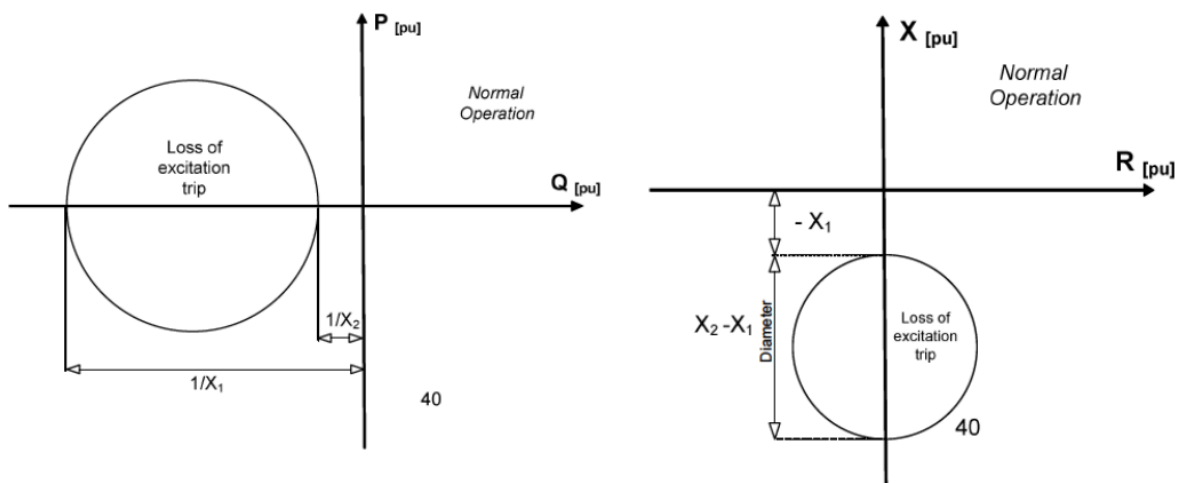


Figure 19. Loss of excitation trip areas on a P-Q plot (left) and R-X plot (right) (López, et al., 2017).

Formulas covering the conversion between the PQ-plot and RX-plot are found in appendix 1.

An offset and circle diameter are used to determine the trip area on the plot ( $X_1$  and  $X_2$ ). By combining the illustration on the plots in Figure 19 with the information in Table 3, the trip area for different kinds of generators to both R-X and P-Q plots can be determined. According to López et al., the setting recommendations presented in Table 3 are a result of research of recommendations of numerous manufacturers and scientific articles.  $X_1$  and  $X_2$  consist of different values of the transient direct reactance ( $x_d'$ ) and the synchronous direct reactance ( $x_d$ ) (López, et al., 2017). This method simplifies the transition between the PQ-plot and the RX-plot, allowing determination of settings for both planes.

For example, the underexcitation limits for a salient pole synchronous generator at a hydropower could be set as follows when obtaining the information from row 1 in Table 3:

#### **P-Q**

$$Offset = \frac{1}{X_2} = \frac{1}{0.8 \cdot x_d} \quad (2-34)$$

$$Diameter = \frac{1}{X_1} - \frac{1}{X_2} = \frac{1}{\frac{-x_d'}{2}} - \frac{1}{0.8 \cdot x_d} \quad (2-35)$$

#### **R-X**

$$Offset = -X_1 = \frac{x_d'}{2} \quad (2-36)$$

$$Diameter = X_2 - X_1 = (0.8 \cdot x_d) - \frac{-x_d'}{2} \quad (2-37)$$

Table 3. Loss of excitation setting recommendations (López, et al., 2017).

Settings	$X_1$ [pu]	$X_2$ [pu]
1 Salient pole	$-X_d'/2$	$0.8 X_d$
1 Synchronous motor	$-X_d'/2$	$0.8 X_d$
1 Cylindrical rotor	$-X_d'/2$	$X_d$
2 Any type	$-X_d'/2$	$X_d$
3 Any type	$-X_d'/2$	$(1.1- 1.15) X_d$
4 Any type	$-X_d'/2$	$X_d + X_d'/2$
5 Any type	$-X_d'/2$	$X_d + X_d'/2$
6 Any type	$-X_d'/2$	$X_d$
7 Any type	$-X_d'/2$	$X_d + X_d'/2$

Additional alternative calculations regarding the conversion between the plots are included in appendix 1.

When the capability curve is known, the settings can be defined. Siemens uses three lines, Characteristic 1, 2 and 3, to determine at which points the generator is too underexcited and should trip. A model of the characteristics lines is presented in Figure 20. These three lines are defined by a starting point (a value of  $x_d$ ) and an angle, which are dependable of the generator's stability limits. According to Siemens, Characteristic 1 and 2 are crossed and should be set before or partially on the practical stability curve defined by the capability curve. The starting points and angles should therefore be adjusted accordingly to fulfill the requirements set by the practical stability limit (Siemens, 2020).

As seen in Figure 20, Characteristic curve 3 is further in the underexcitation zone. The purpose of this limit is to protect the machine from exceeding beyond the dynamic stability limit of the generator. If this curve is passed, the generator is in asynchronous operation and should therefore be tripped with a short delay. The dynamic stability limit is very seldom defined in the generator capability curve. Therefore, Siemens has general setting recommendations for Characteristic 3. According to Siemens, a starting point of  $2 \times (1/x_d)$  has proven itself to be a pragmatic procedure in most cases. The angle should represent the inclination of the

dynamic stability limit, but a value of  $100^{\circ}$ - $120^{\circ}$  is considered practical (Siemens, 2020).

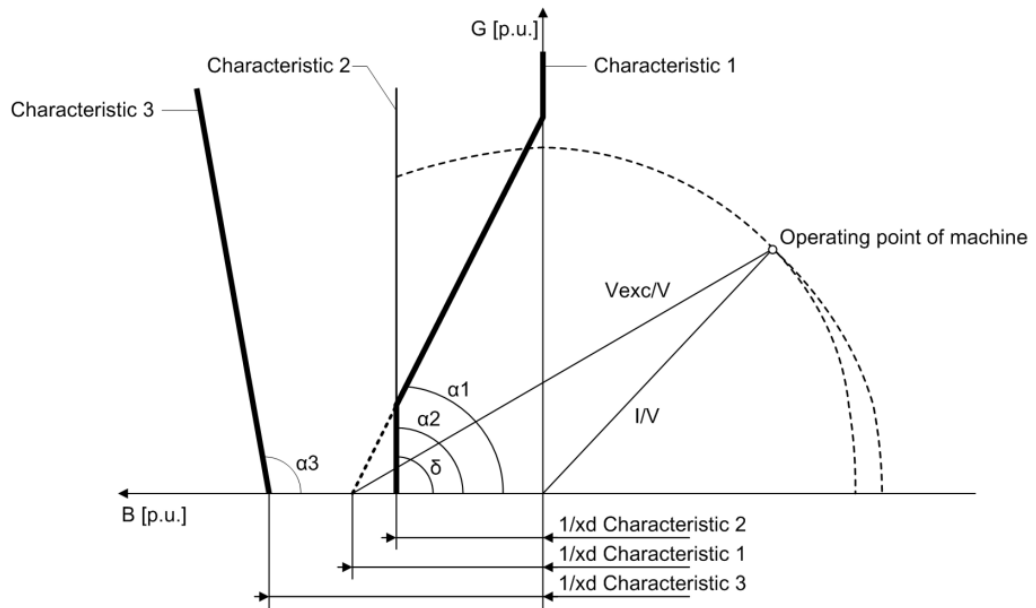


Figure 20. The Characteristics curves of underexcitation protection in the Siemens Siprotec 5 relay (Siemens, 2020).

### 2.3.9 Over-excitation

According to IEEE-standards, if the operation voltage is within 5% above or below the rated value, the generator should be capable to maintain the rated kVA, frequency, and power factor. Overexcitation is one factor that could have an impact whether the machine can operate within the mentioned values or not. Following abnormal operating conditions may often be a sign of an overexcitation: the voltage/frequency ratio exceeds 105% for a generator, 105% for a transformer at full load and 0.8 pf, and 110% at zero load at a transformer's output terminals. Saturation of the generator core and eddy currents in the laminations are the risks, whether overexcitation would occur. Other components may also suffer from damage, especially parts which are not designed to carry any kinds of currents. This fault would eventually result in overheating in the generator and failure in the insulation

(IEEE, 2007).

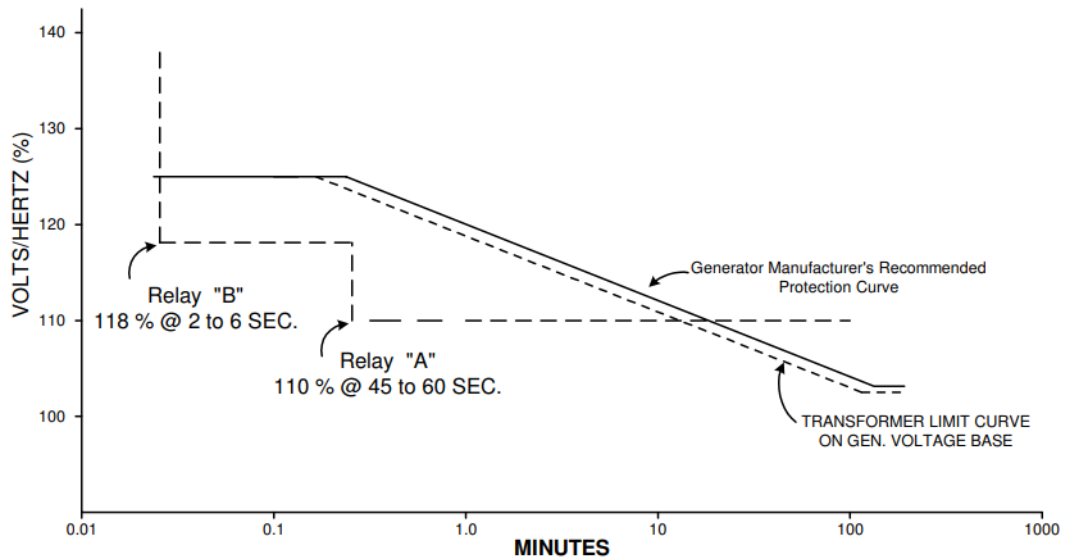


Figure 21. Typical settings for a V/Hz relay (IEEE, 2007).

Figure 21 describes the trip delays when V/Hz ratio exceeds certain limits. General recommendations for the trip delay are 2-6 seconds for a V/Hz ratio of 118%, and 45-60 seconds for 110% (IEEE, 2007). The optimal values may vary from case to case and from machine to machine since these are only recommendations.

### 2.3.10 Undervoltage

Undervoltage relays are used to track the operating voltage level. To maintain the rated power and frequency, the voltage must remain on a level of at least 95% of the generators rated voltage level. Operation below the 95% will increase the amount of reactive power from the grid and reduce the generators stability. Maloperation of equipment sensitive to its voltage supply will also be a result of operating the machine at a too low voltage level. (IEEE, 2007).

The standards regarding undervoltage protection are set by Fingrid. According to Figure 22, normal operation is allowed continuously with voltages of 90 % of the generator nominal voltage. According to standards presented in Figure 22, the maximum voltage for trip must be below 90% of the nominal voltage, and with a trip

delay over 10 seconds ( $U_{TRIP} < 90\% U_{GN}$ ,  $t_{TRIP} > 10$  seconds). The undervoltage settings could for instance be set as follows:

$U_{<}$ , trip value:  $0.85 \times U_{GN}$

Trip delay: 11 s (according to Figure 22)

$U_{<<}$ , trip value:  $0.7 \times U_{GN}$

Trip delay: 1 s (according to Figure 22)

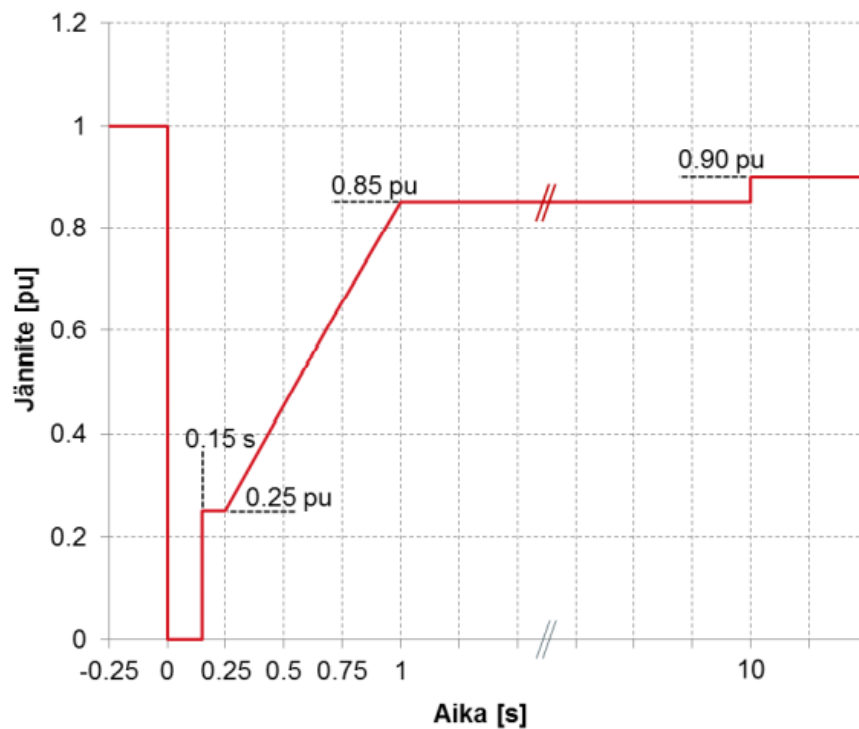


Figure 22. Fingrid's standards for undervoltage trip delay (Fingrid Oyj, 2018).

### 2.3.11 Overvoltage

Overvoltage occurs when the rotation speed for some reason exceeds the rated limits, or when the voltage of the excitation system is too high, even though the excitation current would remain at a normal level. An overvoltage relay is required to detect the exceeded voltages, since the V/Hz relay is unable to detect a fault of this kind. The instantaneous unit scheme is used here to detect overvoltage levels of 130%-150% of the rated voltage level. Additionally, the inverse time unit is often used to detect voltage levels of 110% of the rated value (IEEE, 2007).

The standards regarding overvoltage protection are set by Fingrid. The voltage level can increase to 105% of the generator nominal voltage and still be able to operate normally.

The generator must remain connected to the grid for a minimum of 60 minutes when operating with a 10% increased voltage, as illustrated in Figure 24 ( $U_{TRIP} > 1.1 \times U_{GN}$ ). The stage one trip level should be set slightly above the restricted  $110\% \times U_{GN}$ , approximately with a margin of 5-10% above restriction with a trip delay of couple of seconds. The nominal voltage of the associated medium voltage switchgear must also be taken into consideration when setting the overvoltage values.

The stage two setting should be  $130\% \times U_{GN}$  or upwards, but very seldom above  $150\% \times U_{GN}$ . However, the recommended value by the manufacturer is to be followed here if given. The stage two trip delay is short, approximately a few cycles.

### 2.3.12 Frequency

Abnormal frequencies can disturb the generator operation if the load is rejected, or if the power demand of the grid would not meet the power generated. The frequency of the grid may have minor variations from time to time, depending on whether the ratio between the power demand and power generation is high or low (Fingrid Oyj, 2020). Figure 23 presents the average monthly frequencies of the Nordic synchronous system in 2019. The graph illustrates that the grid kept its stability throughout the year, since only slight variations appeared in 2019. However, single peaks and drops may have occurred since the graph presents only the average values.

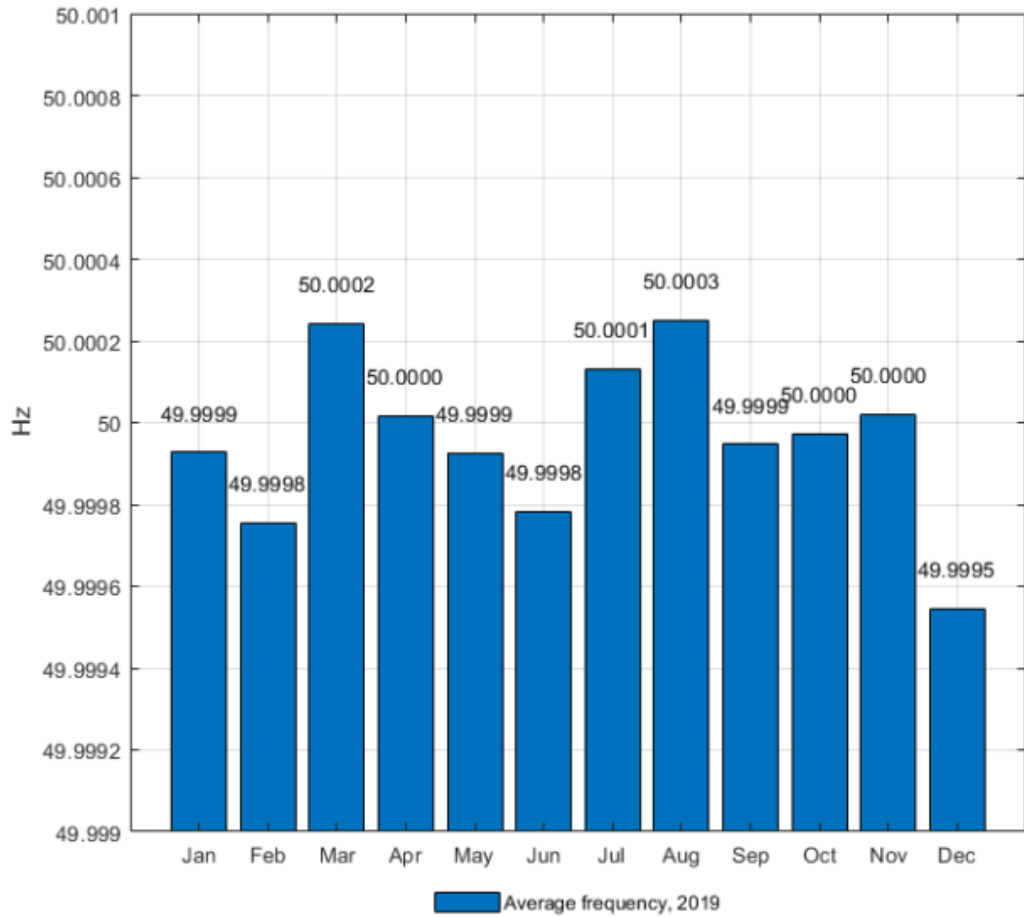


Figure 23. Average monthly grid frequencies of the Nordic synchronous system in 2019 (Fingrid Oyj, 2020).

Operation at increased frequency may occur during load rejection since generators tend to increase the rotation speed during those conditions. Usually, the rotation speed and operation frequency are regulated rapidly back to the nominal values by the generator control system, which often enables continuous operation without any interruptions caused by trips. Underfrequency operation may be a result of a sudden loss of generation, which results in a difference between load and generation. Operation at frequencies below the nominal values may result in a decrease in generator cooling (Mörsky, 1992). Protection against abnormal frequencies is usually the rotation speed control system for the machine or digital or solid-state relays, which can operate accurately, even when covering a wide frequency range (IEEE, 2007).

According to Fingrid, the operation range at Finnish power plants regarding frequency is between 47.5 Hz and 53.0 Hz. Figure 24 describes the range of the values in more detail, including the fact that the frequency may increase or decrease by 1 Hz from the nominal 50 Hz at any time during normal operation. For at least 30 minutes, the generator must remain online when operating in the range between 47.5-51.5 Hz ( $f_{TRIP} < 47.5 \text{ Hz}$  and  $f_{TRIP} > 51.5 \text{ Hz}$ ). For example, 52 Hz and 47 Hz could be optimal values for these settings at stage 1. The minimum frequency requirements by Fingrid cannot blindly be set for all generators since some machines might have stricter requirements regarding low frequencies. Fingrid requirements only apply while connected to the grid, which means that offline generators should follow restrictions set by the generator manufacturer.

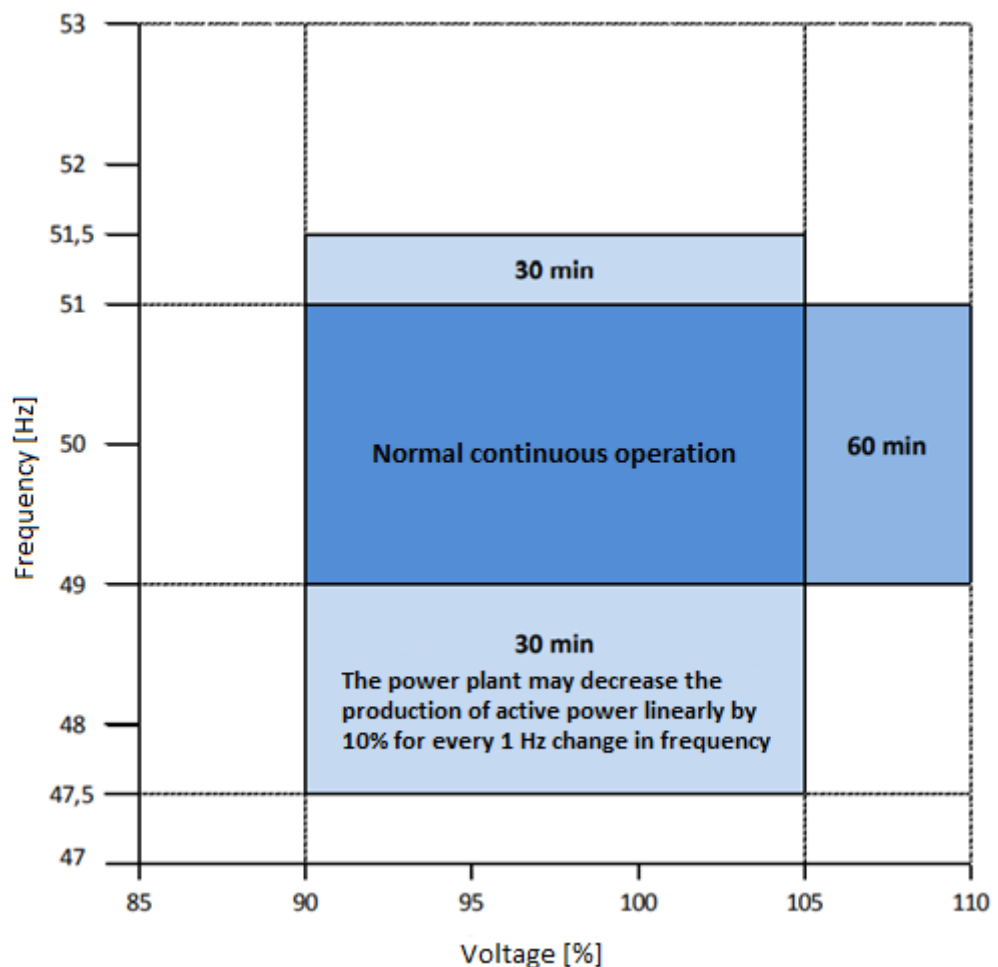


Figure 24. Operational ranges for frequency and voltage at power plants connected to the Finnish power grid (Fingrid Oyj, 2018; modified).

### 2.3.13 Reverse power

Generator motoring occurs at hydropower plants, when water flow to the turbine is for some reason shut down when the generator remains online. This results in the generator to behave as a synchronous motor and will therefore drive the turbine as a pump. In these cases, the turbine is the component that might suffer from damage if motoring, or reverse power flow, would occur (IEEE, 2007).

A power relay is used to detect reverse power situations. The levels of reverse power can be high, when the turbine blades are below the tail-race water level, and when above, the reverse power may only be 0.2%-2% of the rated power level. The sensitivity of the relay can therefore be lower at power plants where the blades are under the tail-race water level, and higher where they are above it (IEEE, 2007).

Motoring power is 0.2-2% for hydro turbines with blades above the tailrace level and of water and >2% when blades are under or at the level (Ferguson, 2016). This is confirmed by an article from Finney et al. (2017). This means that most applications with Kaplan and Francis turbines reach a motoring power of <2%, and power plants with Pelton turbines a percentage of >2%.

$$P_m = \frac{\%P_m \cdot S_{GN}}{CT_{RATIO} \cdot VT_{RATIO} \cdot 3} \quad (2-38)$$

where  $P_m$  is the motoring power per phase (W),  $\%P_m$  is the motoring power percent for a specific turbine type and  $S_{GN}$  is the generator nominal apparent power (VA). The trip delay setting is usually 5-10 seconds for reverse power protection. (Mowat, 2010).

### 2.3.14 Shaft current

Shaft current protection is required to protect the bearings from the high temperatures that occur when the current flowing in the shaft becomes too large. The shaft currents are detected by a current transformer attached to the shaft as presented in Figure 25. Shaft current protection is usually applied on salient-pole generators at hydropower plants. The protection is especially important at applications where the shafts are relatively long, which often tend to be the case at hydropower plants. Magnetic fields and friction are possible causes of voltage in the shaft, causing it to become a potential voltage source.

Relatively high currents may damage the bearings since they are grounded, which means a closed circuit. According to Siemens, greater currents than 1A are often critical for the bearings and may damage and weaken them rapidly. Therefore, the current setting should be set below 1 A (Siemens, 2020). The number of secondary winding-turns is dependable on the shaft diameter but is usually around 400-1000 turns.

The shaft current should initially be measured at normal operation conditions, in order to determine the optimal current setting. If no measurement data is available, a setting below 1 A with a safety margin is a decent value for most applications. Siemens recommends a trip delay of 3 seconds, to avoid unnecessary trips due to minor disturbances.

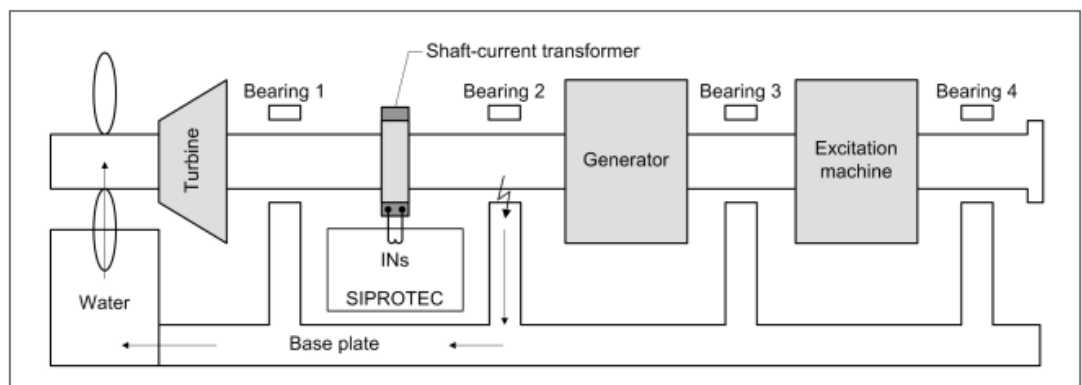


Figure 25. Placement of the Shaft-current transformer and possible flow of fault current (Siemens, 2020).

### 2.3.15 Out-of-step, pole slip

Low levels of generator excitation, low operating voltage, or high impedance levels between the machine and the remaining system reasons for loss of synchronism to occur. During this abnormal operating condition, high current peaks and out-of-step frequency operation occurs, eventually resulting in torque pulses and overload stress on windings. Immediate trip is preferred during these conditions, since not much time is required for the machine and the shaft that connects the turbine with the machine to suffer from damage. Separate relaying to protect the machine against loss of synchronism is required, since differential relays and time-delay schemes cannot detect loss of synchronism. However, relays that detect the loss of excitation may track the synchronism losses to a certain point, but not to a level where it can be fully trusted (IEEE, 2007). Impedance variations relaying can be utilized to detect loss of synchronism.

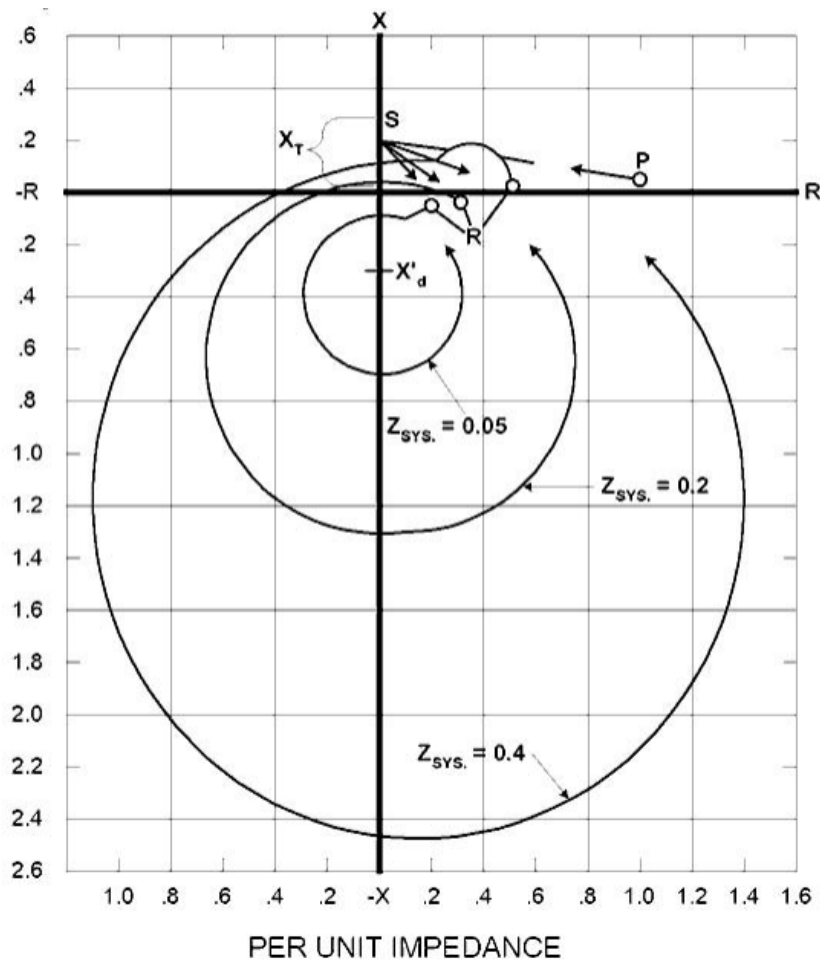


Figure 26. Loss of synchronism due to impedance variations (IEEE, 2007).

Figure 26 presents the loss of synchronism due to impedance variations from the generator terminals' point of view. The impedance variations are approximated by the circular characteristics, as shown in the Figure. In the graph, P means the load impedance initially, S is the short-circuit impedance, R the clearing point, and  $Z_{SYS}$  is the system impedance (IEEE, 2007).

### 2.3.16 Breaker failure

The generator breaker is the device that trips the machine during faults of such magnitude when trip is required. A timer is used to detect if the breaker trips the unit or not within the timeframe set in the timer. The scheme to detect the position of the breaker can include current measurement or an auxiliary contact that detects the position mechanically. If a signal of breaker failure is received from one of the sensors, additional protection equipment will trip the unit (IEEE, 2007).

The timer setting consists of the measured mechanical operation time of the breaker, the breaker failure function drop-out time, delay within the relay software, and a time multiplier depending on how much delay is allowed. The time multiplier is used to find the balance between unnecessary trips and damage on equipment caused by pushing the trip delay too far. The drop-out time can be found in the relay user manual.

Atienza and Moxley presents the clearing times to be considered when determining in their article "Improving Breaker Failure Clearing Times" from 2011 in Table 4. Using a relatively modern breaker with traditional scheme, the maximum breaker failure clearing time is estimated to be 224.51 milliseconds. A timer delay of 300–400 ms could therefore be an optimal setting for most applications. However, the lifespan and age of the power plant and its equipment should be taken into consideration when setting the timer delay, since breakers that has been in operation a longer time tend to suffer from more mechanical inertia than newer and more modern ones (Atienza & Moxley, 2011).

In order to reduce the breaker failure clearing times and to implement the optimal

breaker failure schemes, Atienza and Moxley recommends using high-speed contacts in advanced relays, since their research shows that it is more economically beneficial to replace relays to newer ones, than to replace three-cycle breaker with two-cycle breaker. Other recommendations are utilization of multifunctional differential and distance relays, which include breaker failure protection, and the usage of ethernet communication to reduce the clearing times even further. Regular service on the breaker is also important in order to avoid major increasement in the mechanical inertia, and therefore increasement in the clearing times (Atienza & Moxley, 2011).

Table 4. Breaker failure clearing times (Atienza & Moxley, 2011).

	Traditional Scheme		Traditional Scheme With Two-Cycle Circuit Breakers		Traditional Scheme With Advanced Relaying		Traditional Scheme With Two-Cycle Circuit Breakers and Advanced Relaying	
	cycles	ms	cycles	ms	cycles	ms	cycles	ms
<b>Primary Protective Relay Data</b>								
Maximum Distance Relay Operate Time 70% of Zone 1 Reach, SIR = 1	1.500	25.00	1.500	25.00	0.800	13.33	0.800	13.33
Trip Output Contacts	0.360	6.00	0.360	6.00	0.060	1.00	0.060	1.00
Breaker Failure Initiate Output Contact	0.360	6.00	0.360	6.00	0.060	1.00	0.060	1.00
<b>Circuit Breaker Data</b>								
Maximum Circuit Breaker Clearing	3.000	50.00	2.000	33.33	3.000	50.00	2.000	33.33
<b>Breaker Failure Relay Data</b>								
Open-Phase Detection	1.500	25.00	1.500	25.00	1.000	16.67	1.000	16.67
Security Margin	2.000	33.33	2.000	33.33	2.000	33.33	2.000	33.33
Breaker Failure Relay Input Debounce Timer	0.500	8.33	0.500	8.33	0.250	4.17	0.250	4.17
Breaker Failure Relay Processing Interval	0.250	4.17	0.250	4.17	0.125	2.08	0.125	2.08
Breaker Failure Pickup Delay	6.500	108.34	5.500	91.67	5.875	97.92	4.875	81.25
Breaker Failure Output Contact	0.360	6.00	0.360	6.00	0.060	1.00	0.060	1.00
<b>Lockout Relay Data</b>								
Lockout Operate Time	1.000	16.67	1.000	16.67	0.500	8.33	0.500	8.33
<b>Local and Remote Circuit Breaker Data</b>								
Maximum Circuit Breaker Clearing	3.000	50.00	2.000	33.33	3.000	50.00	2.000	33.33
<b>Maximum Breaker Failure Clearing Time</b>	<b>13.470</b>	<b>224.51</b>	<b>11.470</b>	<b>191.17</b>	<b>10.670</b>	<b>177.83</b>	<b>8.670</b>	<b>144.49</b>

## 2.4 Generator protection relays

Examples of common protection relays used at hydropower plants in the company's projects today are the Siemens Siprotec 7UM85, Arcteq AQ-257, Schneider Electric Easergy P3G30/PrG32, ABBREG630 and VAMP 210, which are presented in Figure 27.



*Figure 27. The Siemens Siprotec 7UM85 (Siemens, 2020), Arcteq AQ-257 (Arcteq, 2018), Electric Easergy P3G30/PrG32 (Schneider Electric, 2017), ABB REG630 (ABB, 2019) and VAMP 210 (Schneider Electric, 2018) protection relays.*

To conclude the requirements for generator protection relays, the protection functions should be selective in a way that only certain sections of the system would remain offline when a fault occurs. Also, the automatic measures should be executed without delays to minimize the disturbances, damage and danger caused by a fault. The relays should preferably have relatively simple user interfaces to ensure secure operation of the system (Mörsky, 1992).

### **3 MATERIAL AND METHODS**

This section covers the process of tests and comparisons the calculation software tools. Tools and functions available in the demo versions will be tested and evaluated. Unfortunately, demo versions seldom have all tools unlocked for the user. This means that the full picture of the offered properties will not be experienced.

The software is aimed to assist the user to obtain data from the power generation process and to function as support when setting the relay settings.

#### **3.1 Simulation software**

The three software tools chosen for the thesis are Powerfactory Digsilent, ETAP and Siemens PSS/CAPE. The choices are based on overall impressions over the software and availability of demo and test versions. Different simulation and protection setting tools are studied, evaluated and compared. Notable here is that the demo licenses include fewer tools and functions than the complete versions, which must be included in the evaluations of the specific software. This kind of software was found to be relatively complex during the tests and simulations, which made it challenging to fully explore the features and tools. However, all three of the software included similar tools which could be compared.

In this section, methods used for test and comparison of the software are described in detail. A hydropower plant with 3 turbines is used as model for the simulations. Two generators have a nominal apparent power of 53 MVA, while the third operates nominally at 25 MVA. The power factor of all the machines is 0.9, resulting in an active power of 47.7 MW for the larger machines, and 22.5 MW for the third one. The powerplant operates at three voltage levels, of which 0.4 kV, the low voltage section, is used to produce the power for self-use at the power plant. The generators operate at a nominal voltage of 10.5 kV, which is the medium voltage section in the system. The medium voltage is then transformed to the 110 kV grid voltage through the unit transformers.

Load flow, short circuit, and time-overcurrent simulations are tested to some extent for all the software. Additionally, some simulations which calculates and suggests relay settings is also tested, but this kind of feature was only found to be available for the PSS/CAPE software.

The goal is to reach similar values of power flows and short circuit currents between the software in the above-mentioned simulations and to analyze possible differences.

Powerfactory Digsilent is used for simulation and modelling of different generation, distribution and transmission applications. The tools can both be utilized at the planning stage of an application, while sizing, or when simulating and modelling existing grid operation. Powerfactory Digsilent provides analysis of both mechanical and electrical behavior at different conditions. In addition to technical analysis, operations cost calculations can also be simulated within the software. Models of generators, governors and protection relays alongside a relay library are also included (DIgSILENT, 2022b).

ETAP also features different simulation tools for a variation of network applications. Power plants, distribution networks and industrial applications are the main areas of focus in the software. The user is allowed to choose from a selection of different modules of the software based on the user's needs. The features of the different modules vary whether the user is interested in power plant or distribution network simulations (ETAP, 2020).

Siemens PSS/CAPE is a simulation software specialized in protection. Different faults can be applied at certain locations in the system and analyzed through different plots and graphs. The wide range of the software's relay model library and protection tools enable the management of complex network data. Certain functions are included in the standard module, but several optional features may be added as needed. The relay setting module calculates relay settings through user-written macros or basic macros which are included by default (Siemens, 2021).

## 3.2 Simulations

In this section, the simulations are presented visually and verbally one software at a time, followed by comparisons and analyses of the obtained data and impressions.

### 3.2.1 Powerfactory Digsilent

A new project must initially be created to be able to design the power plant. Some data are requested at the start, mainly regarding the network frequency, units and which standards are preferred. The design of the power plant worked well since a wide range of symbols was available, for example different types of generation units, transformers, loads, and circuit breakers. It was relatively simple and effortless to draw and connect the different sections of the system. The design of the single-line diagram of the system is presented in Appendix 2.

The load flow simulation presents the power and current flows through the branches and busbars in the system. Figure 28 presents the different load flows through the system when the generator, G3, is operating at 100% power. The complete load flow simulation is presented in Appendix 3. The software uses colors and percentages to describe the relative loads on different components and sections. For example, G3 from Figure 28 is visualized as red when the load is 100%. The presented data here is active power, reactive power, and current in the lines, and voltage in kV and per unit alongside the phase angle shift. The data presented is customizable to some extent. The load flow simulation is a practical tool when dimensioning and sizing different sections of the system, as the user quickly recognizes any flaws or weaknesses.

The percentages are highly dependent of the input data, which means that minor variations of some parameters might cause the software to present false and misleading results.

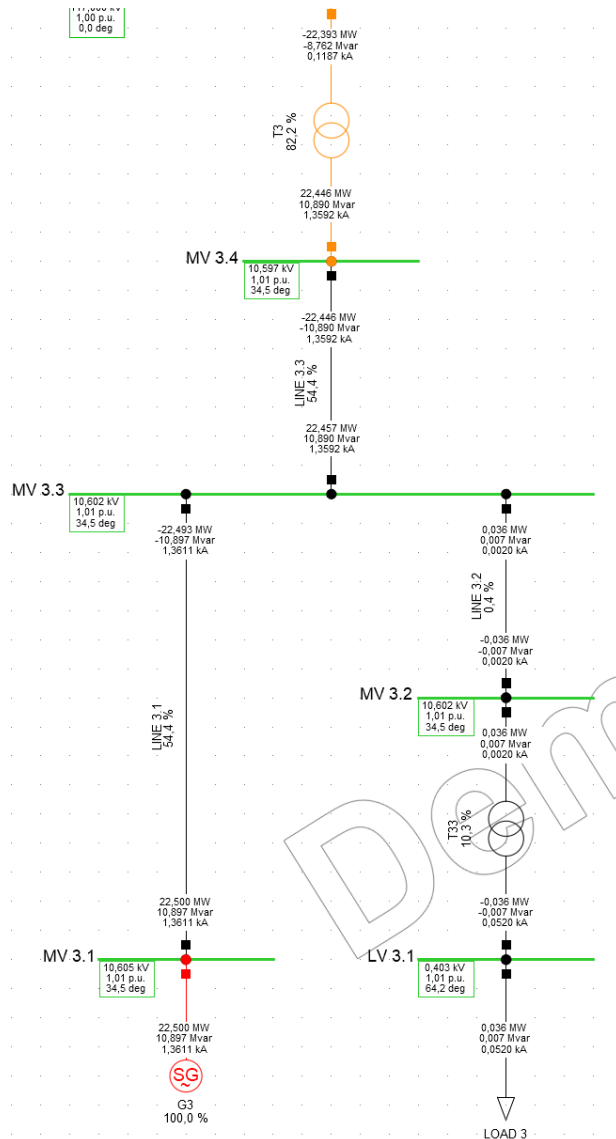


Figure 28. Load flow simulation in Powerfactory Digsilent (Digsilent, 2022a; modified).

Another simulation tested in the software was the short circuit simulations. Different kinds of faults may be applied to the desired location to simulate how the system responds. In this study, maximum three-phase, minimum three-phase and minimum two-phase faults were simulated. Figure 29 presents the different simulation values at the G3 branch when the faults were applied at the busbars. The data presented is the initial short circuit power in MVA, initial short circuit current in kA, and peak short circuit current in kA. The currents displayed in the minimum two-phase short circuit simulation is the initial short circuit currents of the two faulty phases. The short circuit simulations were calculated by the IEC 60909 standard. The complete

simulations are presented in Appendices 4-6.

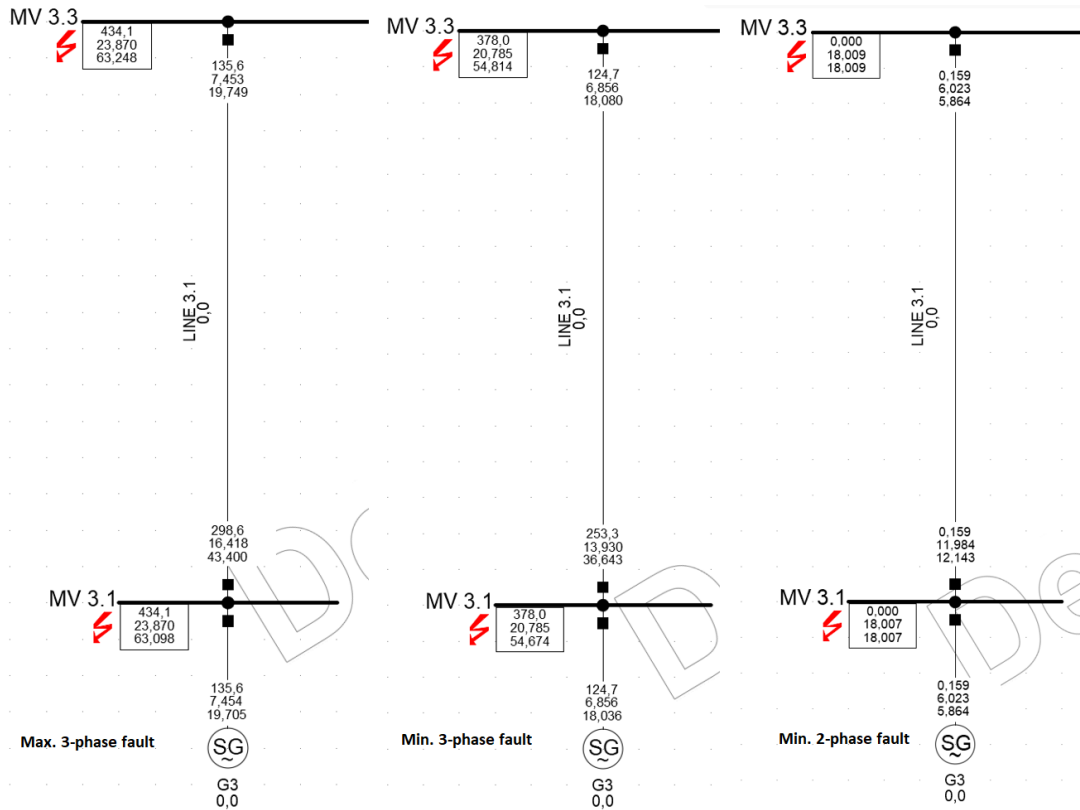


Figure 29. Short circuit simulations in Powerfactory Digsilent (Digsilent, 2022a; modified).

Time-overcurrent plots were also drafted and simulated. These graphs are useful when testing whether overcurrent settings are set properly or not. Figure 30 illustrates the overcurrent protection set for G3 during 100% load conditions with the time in seconds on the vertical axis, and the primary current in A on the horizontal axis. The time-overcurrent curve illustrates the duration for how long different magnitudes of currents are allowed to operate before tripping the machine.

The vertical line represents the nominal load current, which is 1.36 kA in this case. The curves on the right hand represents the time-overcurrent protection curve, which is a combination of IEC Normal Inverse curve and a Definite Time zone. This means the trip time decreases when the current increases. This is only until a certain point, where any current greater than that will trip with the given trip delay. The pickup value for Definite Time zone here is four times the generators nominal current, which equals 5.5 kA, while time setting is set to 0.04 s. As seen in the plot, the

nominal load condition current will not cause a trip since the vertical line is not crossing the time-overcurrent curve.

The software allows the user to set different combinations of overcurrent protection, a two stage Definite Time protection with different trip times is another alternative.

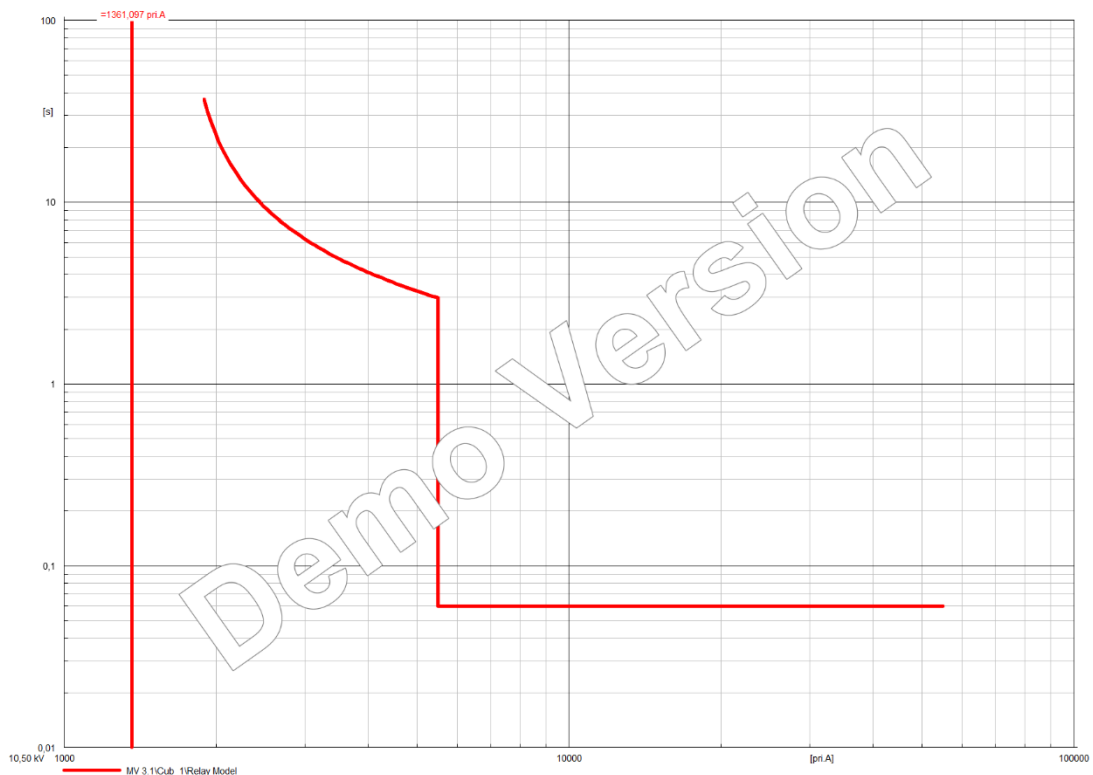


Figure 30. A user-defined overcurrent protection scheme in Powerfactory Digsilent (Digsilent, 2022a; modified).

The next step was to apply a fault to simulate the trip time for the relay. As mentioned before, the minimum two-phase short circuit current must be tested here since that is the minimum value of current that must always cause a trip. According to Figure 31, the overcurrent settings here do cover the minimum fault current. This means that the 5.5 kA pickup current would fulfill the criteria in this case.

The software allows the user to simply right-click on the anywhere on the time-overcurrent curve to determine the trip delay times at a certain value of current.

Furthermore, the software can also illustrate a capability curve of a generator, which

is presented in Appendix 7.

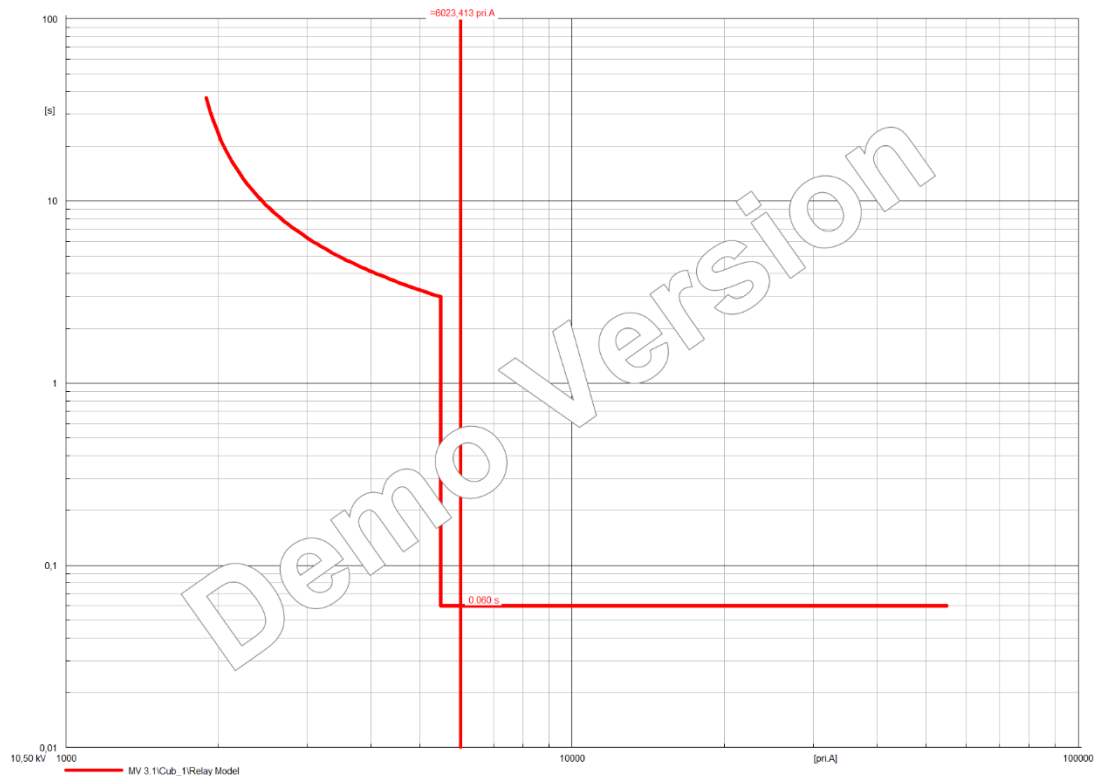


Figure 31. Minimum 2-phase short circuit current simulated in the time-overcurrent plot (Digsilent, 2022a; modified).

### 3.2.2 ETAP

ETAP required similar initial data at the start of a new project as Powerfactory Digsilent. The IEC standards were selected as the standard preferences. The demo version itself was slightly more restricted since some tools are only unlocked in the complete version of the software. The limitations were not directly a surprise since it was expected from the beginning that none of the software would entirely match the full versions. The purpose of the demo versions is to get familiar with the software and its functions. However, the basic simulations could still be completed in ETAP.

The design of the model power plant could not be drawn entirely since the number of busbars was limited in the demo. The only branch drawn here was the G3 branch, but that was still enough to run the simulations. The simulation results are however affected slightly, which will be discussed later.

Figure 32 presents the results of the load flow simulation. Both branches are the same in the figure, left side presents the load flow in apparent power and current, while right side presents active and reactive power. The bus voltage is shown in both variants.

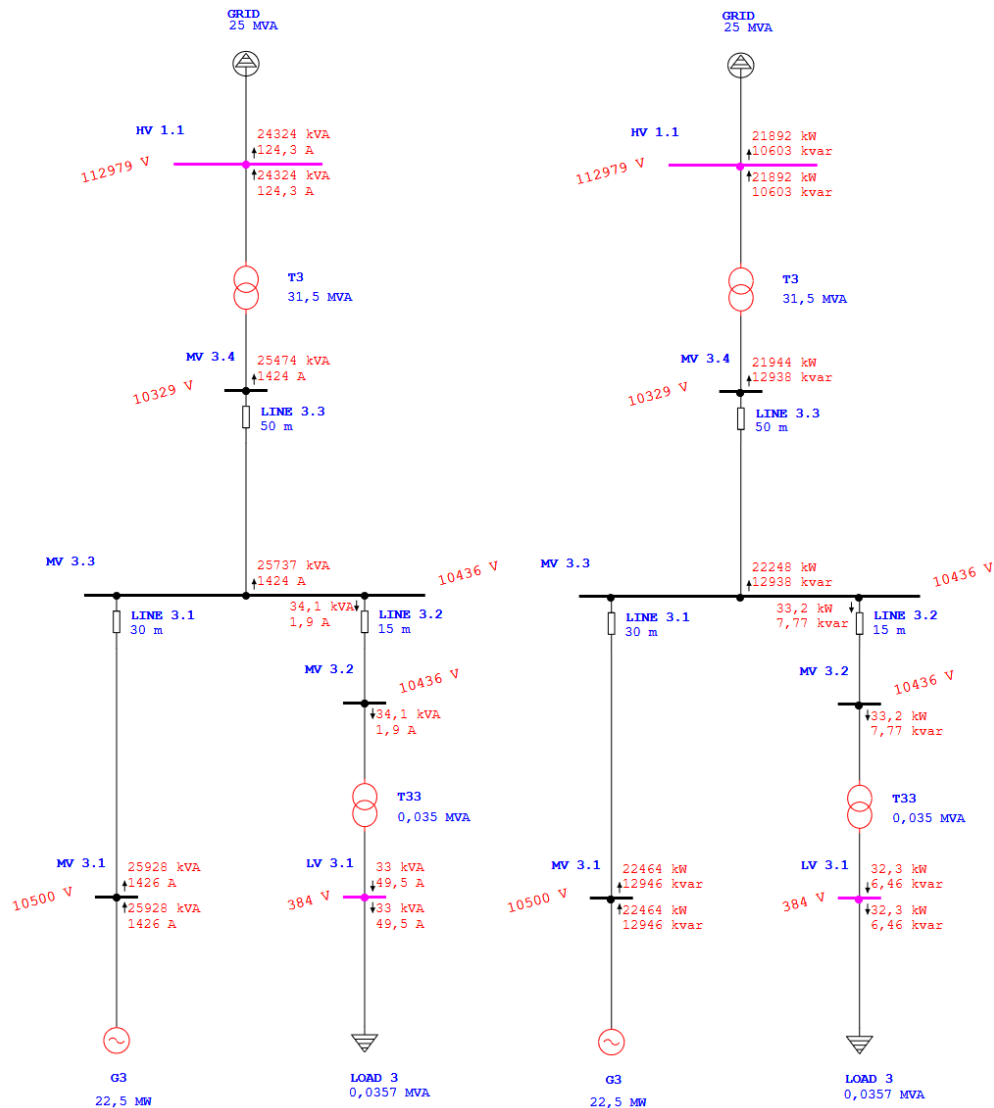


Figure 32. Load flow simulation in ETAP (ETAP, 2022; modified).

The grid load was set to match the MVA-rating of the generator. This caused the generator to operate slightly above its nominal values, due to losses in the lines and the transformer between the grid and the machine. The load flow simulation calculates the apparent, active and reactive power flows through the system, the current, and the busbar voltages. Busbars HV 1.1 and LV 3.1 are colored pink due to

decreased voltages at the busbars. As presented in Figure 32, the apparent power and current from the generator have exceeded the nominal values due to the high load. Interesting here is, that active power is slightly below the nominal 25 MW, while the reactive power is 2 MVAR above the nominal value.

The maximum and minimum three-phase short circuit currents were simulated as shown in Figure 33. The software calculated the initial short circuit current, which is presented in kA alongside the phase angle. The two-phase minimum simulation could not be found in the software, which might be another restriction in the demo version. The faults are applied at every busbar, which indicate the red color.

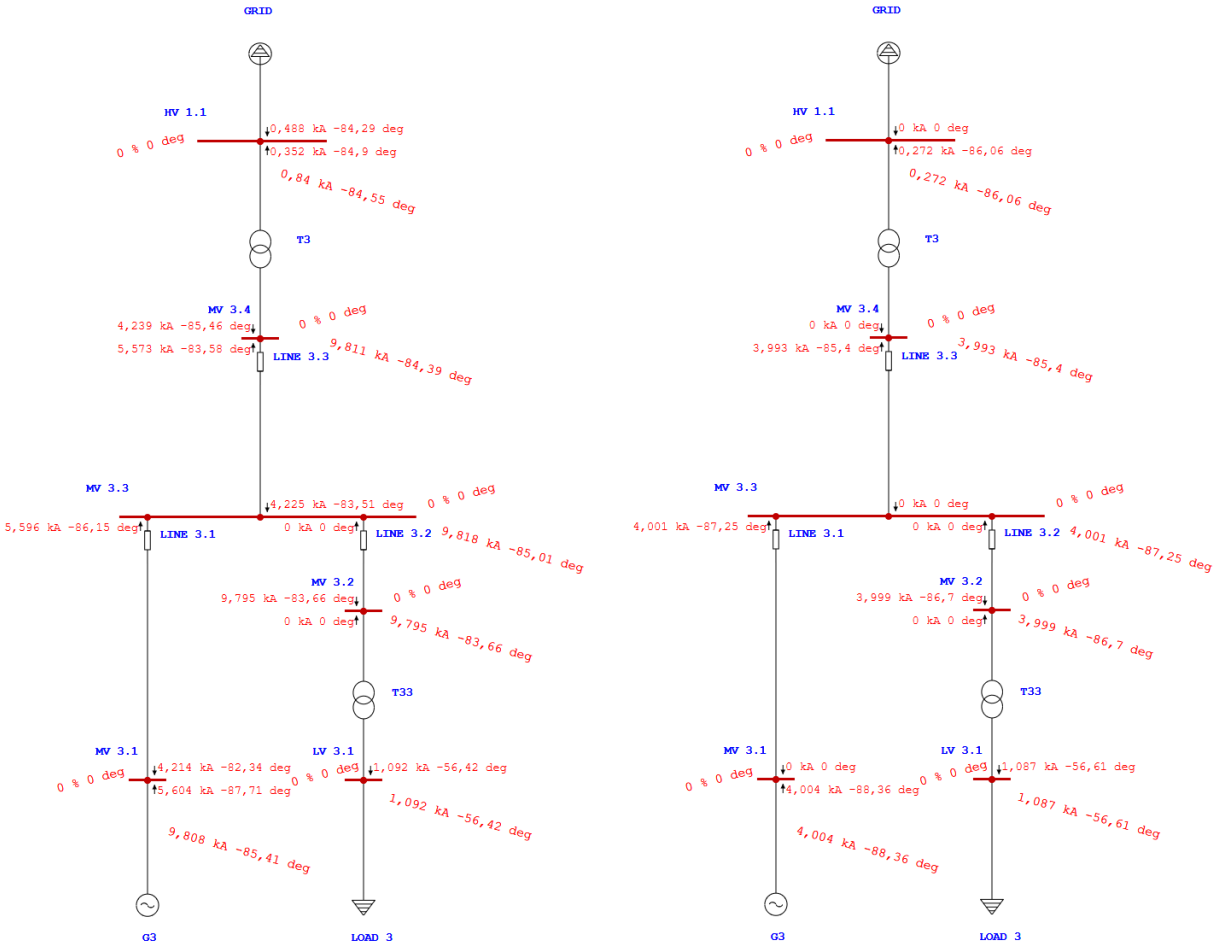


Figure 33. Short circuit simulations in ETAP (ETAP, 2022; modified).

The time-overcurrent simulation could only be performed with a demo relay with the

settings defined by default. The curve is presented quite differently compared to the other software. As shown in Figure 34, the vertical axis represents time in seconds, and the horizontal axis represents the current in A. The two marks on the curve describe the trip delay for 1.2 and 4 times the nominal current, which equal 3.8 seconds and 0.04 seconds with the default settings. The user can see the exact trip delay times at any value of current on the curve.

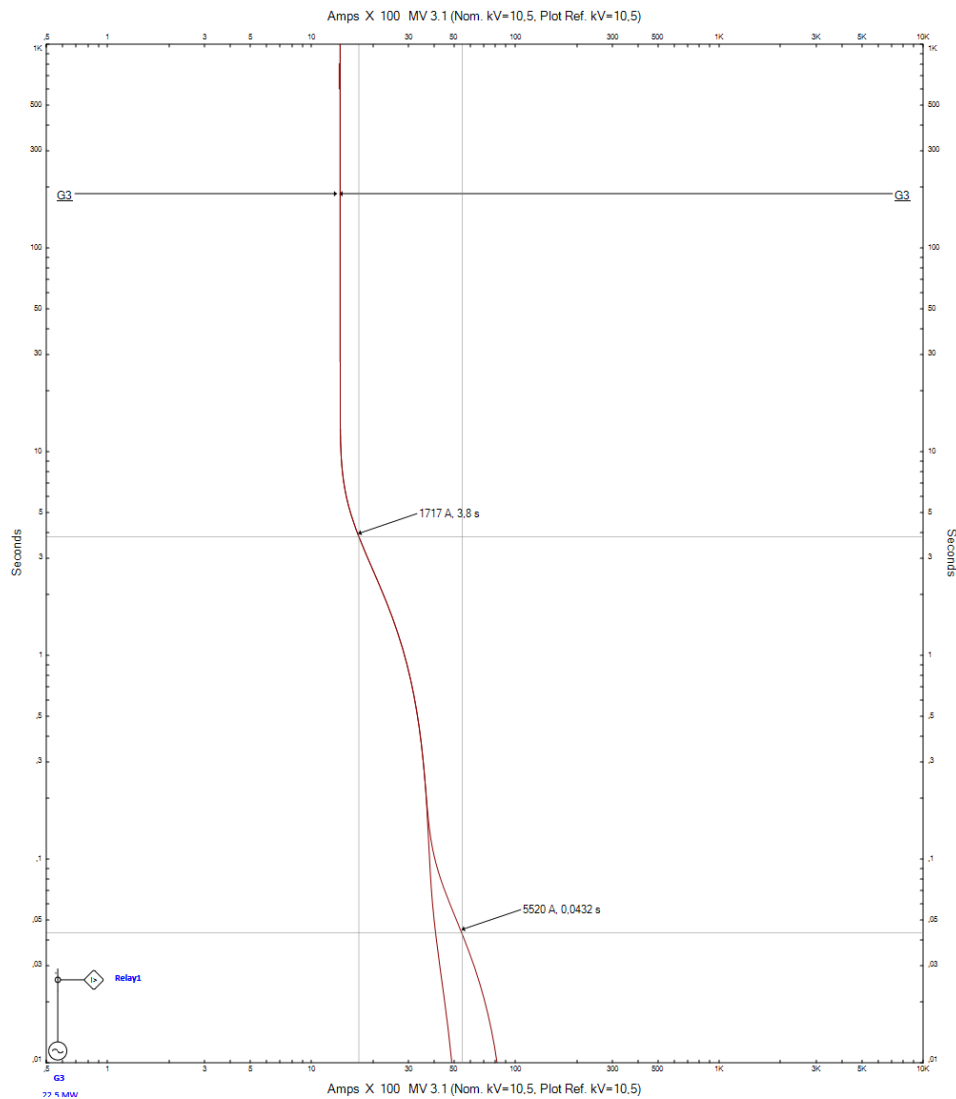


Figure 34. Time-overcurrent simulation in ETAP (ETAP, 2022; modified).

The software was also able to plot the generator capability curve, but for some reason only on the over-excitation side of the diagram, which is presented in Appendix 8. This may be due to some unlocked features in the demo version, or missing input data.

As mentioned above, the results of the simulations were slightly affected by the restrictions in this software, but the important thing is that the simulations needed could be tested.

### 3.2.3 Siemens PSS/CAPE

In addition to create a new project in PSS/CAPE, a separate database must be attached in order to do anything. Every modification in the project will be saved in the database, for instance relay settings. The user can choose whether to create a new database or attach a standard database included in the software and go on from that. After starting a new project, attaching the database, and selecting which standards are preferred in the project, the single-line design of the power plant was drawn, and the load flow calculations simulated according to Appendix 9. Also, the IEC standards were selected as the standard preferences. The G3 branch is presented in Figure 35.

The drawing of the power plant design felt quite clumsy at the start since it took some time to figure out how to place and move different objects in the single-line diagram. Copying of symbols was disabled which resulted in a longer drawing phase timewise.

The load flow simulation presents the active and reactive powers at the lines and the busbar voltages in kV and p.u. The high voltage side is displayed a red, but no other coloring or load percentage was presented in the simulation. As shown in appendix 9, G3 is operated at 100% load, while G2 and G1 are slightly away from the nominal values. This is because symbol for background grid was found in the single-line diagram toolbox.

The background grid has the function to balance the grid to allow all the machines to operate at 100% load, while the loads are receiving their nominal power. Without the background grid, G2 must push slightly beyond its nominal power in this case.

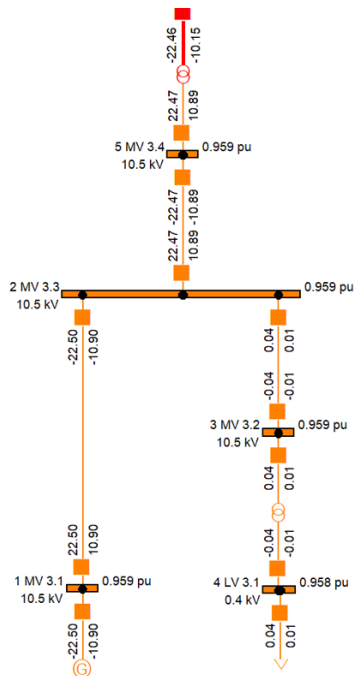


Figure 35. Load flow simulation in Siemens PSS/CAPE (Siemens, 2022; modified).

The remaining simulations were performed through a default demo project included in the software, due to unknown errors in the database settings in the new project. The short circuit simulations were performed at a 115k kV busbar in a three-phase and double-line to ground simulations. The fault currents with angles are presented in the simulation view. The results of the short circuit simulations are presented in Figure 36.

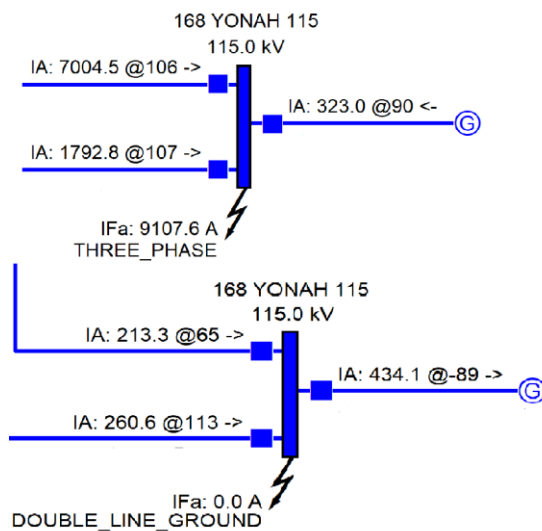


Figure 36. Short circuit simulations in Siemens PSS/CAPE (Siemens, 2022; modified).

The time-overcurrent simulation was simulated through a demo relay as shown in Figure 37. The overcurrent setting here was a combination of a Very Inverse Time curve as the slower protection stage, and a Definite Time zone for the fast trip. The vertical axis shows the time in cycles by default, and the current in A on the horizontal axis. The user-defined marks show the exact time delays at two different locations on the curve. The plot also calculates the difference between the two marks in current and time.

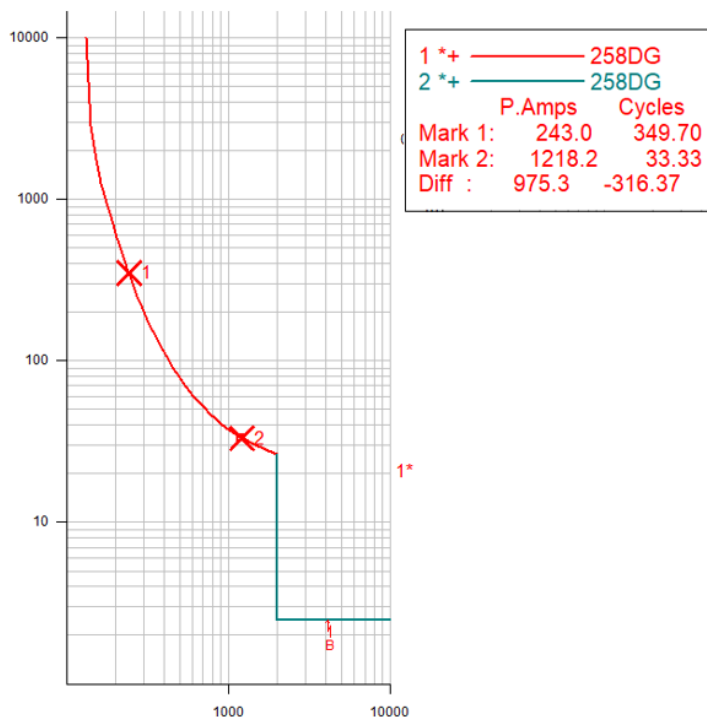


Figure 37. Time-overcurrent simulation in Siemens PSS/CAPE (Siemens, 2022; modified).

The PSS/CAPE software also included a relay setting simulation tool. Relays can be chosen from the relay library alongside an algorithm which automatically calculates the relay settings for the specific protection function. The software includes standard algorithms for different relays, but they can also be user-defined and saved to the relay. A few standard algorithms were tested on a demo relay in the demo project, as presented in Table 5. The demo relay consisted mostly of algorithms regarding current elements.

The demo relay in this case was a Schweitzer SEL-321. The protection functions in

the algorithm were the phase-to-phase overcurrent 50PP, the ground distance phase overcurrent 50L, and the ground distance residual overcurrent 50G. The unit for the pickup value for all the functions is secondary Amperes. The number after the function describes the protection level. The database column in the table shows the default setting in the relay, which in this case is the minimum setting. The previous column shows the old setting, but as no calculations were performed before the simulation, the previous setting is the default setting. The proposed column presents the result of the setting calculation through the algorithm, before comparing the value with the min and max columns to check if the calculation is within the function setting range in the relay. If the calculated value is within the range, the software suggests the calculated value. At level 3 in the table, the calculated values are below the minimum setting value of the function, which results in the minimum value to be set as the suggested value for the setting.

*Table 5. Relay setting simulation in Siemens PSS/CAPE (Siemens, 2022; modified).*

	Database	Previous	Proposed	Min	Max	Set as	
Level 1 (phase elements restricted by load)							
50PP1	1.00	1.00	21.30	1.00	170.00	21.30	Modified
50L1	0.50	0.50	8.35	0.50	100.00	8.35	Modified
50G1	0.50	0.50	6.31	0.50	100.00	6.31	Modified
Level 2 (not restricted by load)							
50PP2	1.00	1.00	13.22	1.00	170.00	13.22	Modified
50L2	0.50	0.50	6.70	0.50	100.00	6.70	Modified
50G2	0.50	0.50	5.17	0.50	100.00	5.17	Modified
Minimum taps for level 3							
50PP3	1.00	1.00	0.31	1.00	170.00	1.00	Raised to min
50L3	0.50	0.50	0.31	0.50	100.00	0.50	Raised to min
50G3	0.50	0.50	0.31	0.50	100.00	0.50	Raised to min

## 4 RESULTS

Several simulations were successfully completed in each software. However, the powerplant layouts were not completely identical, which leads to some challenges in the comparison of the results. Differences between the software were recognized during different simulations and when different tools and functions were explored.

The information from generator, transformer, and cable datasheets was detailed enough to fulfill the input data requirements to be able to run the simulations. The level of detail in the input data was considered quite similar in each software, with minor differences.

The drawing experience in the one-line diagram were quite different between the software in how smoothly and rapidly the designs were produced. Powerfactory Digsilent was considered the best software of the three candidates regarding single-line design, due to its wide range of symbols and availability to copy and paste certain sections of the design. The connection between busbars and components was simple to set up when compared to the other two. Different users might prefer different details and properties, but the Digsilent Powerfactory single-line drawing required the least time to figure out in this study. The possibility to create and modify designs in projects quickly is relatively important in this kind of software, where changes and improvements could be common.

Regarding the load flow simulation, each software calculated logical and similar values. The software presented the power flows and currents at the lines, and the voltage levels at the busbars, with an exception in PSS/CAPE, where the currents were not displayed. The currents might have been added in load flow settings, but such settings were not discovered during the simulations. However, each software proved the load flow simulation to be a useful tool to detect imbalances and flaws in the system. PSS/CAPE was the only software using different colors for different voltage levels, but only between the high and medium voltage levels in the study project. The color between medium and low voltage remained unchanged. The

busbars in ETAP and Powerfactory Digsilent changed color when the busbar voltage started to shift away from the nominal value. Powerfactory Digsilent was the only software displaying percentages of the load in generators, transformers, and lines. The color scheme, which represented the percentages, was clear and simple. Appendix 3 presents the color variation from green to red depending on the load at certain locations in the system.

The short circuit simulations were challenging to compare since each software were simulated with different layout, due to the restrictions in ETAP and the technical challenges in the study project in PSS/CAPE. However, the simulations were still successfully completed. The minimum two-phase short circuit simulation is most crucial regarding protection, as described in chapter 2.3, since the calculation result functions as the reference when setting the stage two overcurrent protection. This was unfortunately only simulated in Powerfactory Digsilent, as the simulation was not discovered in the other software. The three-phase short circuit was however simulated in each software. The simulations were performed by applying faults to each busbar in the system. ETAP and Powerfactory Digsilent simulated quite different values, since in ETAP, the fault should have been applied on a single busbar at a time, to receive correct results. Each software included the possibility to switch off circuit breakers in order to simulate different situations. Ground fault simulations were also included in the short circuit tools for each software.

The time-overcurrent simulation was the simulation where least differences were recognized between the software. Although ETAP presented the curves slightly different, the same information and data was gained from the time-overcurrent plot as in the other software. The time-overcurrent plot did not suggest any settings directly, but it is useful to test different settings and to analyze the results before deciding in which direction to change the settings to improve the operation and ensure safety. It was also possible to include time-overcurrent curves from different relays in the same plot to study selectivity, at least in Powerfactory Digsilent and PSS/CAPE.

The capability curve simulations were performed in Powerfactory Digsilent and

ETAP, the feature is not evaluated as important and crucial as the other simulations since the capability curve is often handed over by the generator manufacturer. If this would not be the case, the capability curve simulation could be considered helpful, especially when determining the under-excitation settings. A suggestion for further studies would be to compare and evaluate how precisely the software capability curves agree with generator manufacturer capability curves.

The relay setting feature in PSS/CAPE was a quite unique function since no similar tool was discovered when exploring the demo versions of Powerfactory Digsilent and ETAP. Ideally the simulation suggests the raw relay settings for the user. However, it remains still quite unsure how well the simulation would work in a real project since it is challenging to analyze how well the standard relay algorithms apply in different situations and powerplants. Realistically, ideal algorithms would be obtained by starting with the standard versions and proceed onward with user-defined modifications to ultimately reach an optimal setting calculation simulation. This tool would be practical, but the study gave the impression that this mainly applies on network protection rather than generator protection.

The overall impressions of the different simulations and tools for each software are summarized in Table 6.

*Table 6. Comparison of the simulations and tools tested for the three software.*

Simulation/tool	Digsilent PowerFactory	ETAP	Siemens PSS/CAPE
Design drawing	+++	++	+
Load flow	+++	++	++
Short circuit	+++	++	++
Time-overcurrent	+++	++	+++
Capability curve	++	+	n a
Relay setting	n a	n a	++
User-friendliness	+++	++	++

Scale: impressive (+++); good (++); room for improvement (+); could not be assessed (n a)

ETAP fell slightly behind the other two software during the test process, mainly due to the restrictions in the demo version. Most functions and simulations reached the level of the others, but no feature stood out from the crowd. PSS/CAPE was rich in tools and features, but the software was the most challenging to learn and to figure out how different simulations would be set up. The software has potential, but quite a few tools were explored in the study case due to the software's complexity. Powerfactory Digsilent calculated the most pleasing results all in all, and the software was the quickest one to get a grasp on. User-friendliness, appearance, and the visual result presentation were the most impressive in this software. The demo version did not include a relay setting feature as the PSS/CAPE. The relay libraries were wide in each software, containing several relays from the largest digital relay suppliers on the market, including relays that the company usually uses in projects.

To conclude the results of the study, neither of the software completely fulfilled the company's needs. The optimal software would have calculated the raw generator relay settings. PSS/CAPE could perform setting calculations, but not specifically regarding the generator settings. However, considering the simulations completed and overall impressions, Powerfactory Digsilent performed best overall, and would therefore be the recommendation for the company to investigate further on, if the company would be interested in these more supportive simulations. Each software tested are highly capable to function as support for engineers during relay setting calculation through their versatile simulation tools.

The tests were completed in April and May of 2022 with the following software versions: Powerfactory 2021 (SP3, Demo), ETAP (Version 21, Demo), PSS/CAPE (CAPE 15, Demo).

## 5 DISCUSSION

The evaluation of the results was quite challenging and interesting since besides technical values and data, personal preferences and knowledge affected the results of the simulations and the recommendations to some extent. User-friendliness is a relative measure of quality, which means that different engineers might receive varying results regarding different tools, depending on factors as expertise and personal requirements.

This kind of simulation software are relatively complex and with a time-consuming learning process, which made it quite impossible to get a full grasp of every detail in every software. Therefore, guidelines regarding which simulations would be tested, evaluated, and compared were defined.

Variations in the results were expected since each software had its own detailed functionalities. Identical input data were not required at every stage between the software, which resulted in minor differences in some simulation steps. As mentioned before, each simulation was not executed with identical single-line diagrams, which also affected the results.

The tests were performed one software at a time since it was expected that the method would increase productivity and avoid any confusion which might have occurred if several simulation tools would have been tested simultaneously.

The tests were completed by me alone. Some variations in results could have been reached if several people would have explored the software since different backgrounds of similar studies could have brought different perspectives to the study.

## 6 CONCLUSIONS AND RECOMMENDATIONS

This thesis reached both its goals, both to gather data and knowledge regarding generator relay setting, and to test different simulation software tools and map which would be the most suitable for the company's needs. As mentioned in the results, neither of the three tested software completely fulfilled the company's needs but could still be great options for other purposes.

The tests were completed through demo versions of the three software, which impacted the results to some extent, as mentioned earlier.

Any analysis regarding financial differences between the simulation software was not included in the thesis, which will still have some effect on the consideration process of a possible license purchase.

Whether a simulation software is chosen or not for further evaluation, the company has now gained additional information of available simulation software on the market. The full scope of the software and its features will be unleashed only after gaining a solid amount experience and knowhow of all the details the software has to offer.

Therefore, a recommendation would be to receive training of the software from the manufacturer, in order to accelerate the learning curve of new users, and therefore be able to implement the simulation software as a part of projects.

A recommendation for further studies would possibly be to evaluate other software available on the market, and to find out if more suitable alternatives would be available. Another recommendation would be to evaluate and consider if any of the tested software in this thesis would be suitable for other purposes.

## SVENSK SAMMANFATTNING

Vattenkraft är en förnybar energikälla där grundprincipen är att konvertera vattnets rörelseenergi till elektricitet. Denna process utförs genom att leda de enorma vattenmängderna genom en vattenturbin, vilket i sin tur leder till att en rotationsrörelse bildas i turbinen. De vanligaste turbintyperna i vattenkraften är Kaplan, Francis och Pelton. Dessa typer har olika mekaniska egenskaper, vilket innebär att de är olika effektiva vid olika fallhöjder och vattenflöden. För att föra över denna rotationsenergi till generatoren, monteras en axel mellan turbinen och generatorns rotor. Utöver rotationen, bör rotorn även ha en magnetiseringsström, vilken matas av generatorns magnetiseringssystem. Vid rätt rotationshastighet och magnetiseringsstyrka uppnås ett fenomen som kallas elektromagnetisk induktion, vilket innebär att energin från vattnet har nu blivit konverterad till elektricitet. Denna energi bör ännu omvandlas till rätt spänningsnivå i en transformator för att sedan kunna distribueras till elnätet.

Vattenkraft har redan länge varit en betydelsefull energikälla globalt, eftersom 15–20 % av världens elektricitet har genererats med vattenkraft mellan 1970 och 2015. Enligt prognosen kommer den årliga globala produktionen fortsättningsvis komma stiga, det förväntas en årlig stigning med 3 % fram till år 2030, då den årliga globala vattenkraftsproduktionen förväntas vara 5500–6000 TWh.

Vattenkraften som energiform är potentiell då den är lagrad bakom en dam, men kinetisk då turbinrotationen uppstår. Faktorer som påverkar den lagrade potentiella energin är vattnets fallhöjd, vattenflödet och vattnets densitet.

Som tidigare nämnt är generatoren maskinen där energikonverteringen äger rum. Under drift kan flera typer av fel uppstå någonstans i kraftverket eller nätet, vilket kan leda till att generatoren bör kopplas bort från nätet. Detta sker genom att öppna generatorbrytaren vilket betyder att generatoren då är fysiskt isolerad från resten av anläggningen mot nätet. Fel som kan uppstå vid drift är till exempel kortslutning, jordfel, överbelastning eller att generatoren faller ur det synkrona varvtalet. Både generatortillverkaren och elnätet ställer krav på hur maskinen bör fungera i olika

situationer. Generatortillverkaren ställer ofta krav på maximala värden som generatoren tål, medan elnätet kan även ställa minimikrav som till exempel att produktionen inte får stannas på grund av vissa kortvariga fel från nätets sida.

Generatoren bör skyddas mot dessa fel för att förhindra farliga situationer eller skador på maskinen och dess tillhörande utrustning. Generatorskyddrelä är apparaten som används för att upptäcka dessa fel. Skyddsreläet programmeras enligt standarder, krav och formler med målet att säkerställa en trygg och jämn drift. Rätt balans bör hittas med tanke på inställningarna, så att de inte är för milda, för då riskeras osäker drift. Inställningarna bör inte heller vara för stränga, så inte produktionen stannar i onödan på grund av mindre obetydliga fel. I detta examensarbete har det undersökts vilka standarder och krav som gäller för de olika skyddsfunktionerna.

Skyddsreläerna får sin mätdata från mättransformatorer och på så sätt kan felen och onormala värden räknas och analyseras. Statorjordfelen förhindras genom att mäta spänningen vid generatorns nollpunkt och jämföra det med det inställda värdet. Denna metod möjliggör att 90–95 % av statorlindningarna är skyddade. Alternativt kan 100 % av lindningarna skyddas, men då krävs det en apparat med ströminjektion. Den enklare metoden med 90–95 % brukar vara vanligare i vattenkraftverken.

Rotorjordfelskyddet går däremot ut på att upptäcka läckströmmar mellan rotorlindningarna och axeln, vilket förverkligas genom att mata in en låg ström och jämföra den med returströmmen. Med hjälp av skillnaden i strömmarna uträknas resistansen, vilken är en direkt indikation på isoleringens skick.

Överströmsskyddet förhindrar generatoren att vara i drift vid för höga strömmar i för långa tider. Vanligtvis används det ett belastningsskydd och ett kortslutningsskydd. Belastningsskyddet tillåter överströmmar på ungefär 120–130 % med en karakteristik som ställas av IEC. Dessa karakteristik är kurvor som anger förhållandet mellan överströmmen och bortkopplingstiden. Kortslutningsskyddet fungerar betydligt snabbare, för då ställs värdet på lite under den uträknade minsta möjliga kortslutningsströmmen, med en kort bortkopplingstid.

Med impedansskyddet kan man skydda till exempel både generatoren och transformatorn samtidigt genom att mäta impedansen i nollpunkten. Genom att addera generatorns och transformatorns impedanser, samt impedans på mellanliggande kablar, får man en referenspunkt. Vid fel kommer det uppmätta värdet sjunka under referensvärdet, och därmed upptäcks felet.

Vad gäller spänning och frekvens, måste generatortillverkarens och elnätets krav uppnås. Elnätet ställer krav på hur länge generatoren bör vara kopplad till nätet vid olika situationer, men samtidigt måste generatortillverkarens rekommendationer tas i beaktande.

Med undermagnetiseringsskyddet skyddas generatoren från att övergå till ostabilt läge. Med hjälp av generatorns stabilitetskurva ställs undermagnetiseringsskyddet in, så att generatoren bortkopplas då den är förbi kurvan som anger gränsen för den praktiska stabiliteten. Stabilitetsgränserna kan anges både som förhållandet mellan aktiv effekt och reaktiv effekt, eller som förhållandet mellan resistans och reaktans.

I examensarbetet har det även testats olika simuleringsverktyg för att simulera kraftverk vid olika driftomständigheter. Dessa verktyg och dess funktioner kan vara till hjälp vid bestämning av inställningarna för skyddsfunktionerna. Simuleringsverktygen som testades var Powerfactory Digsilent, ETAP och Siemens PSS/CAPE. Kriterier för testen var olika funktioner samt användarvänlighet. Simuleringstyper som valdes att testas var "Load flow", kortslutningssimuleringar, simulering av överströmskurvor och simulering av generatorns stabilitetskurva.

Värden på olika simuleringar analyserades och jämfördes. På basis av resultaten av simuleringarna ska företaget (VEO) överväga anskaffning av licenser för det program som anses mest lämpligt. Ekonomiska variationer analyserades inte under examensarbetet, vilket innebär ett ytterligare element att överväga. Testen utfördes med demo-licenser för diverse verktyg, vilket även bör beaktas vid analys av resultat, för att olika verktyg hade olika begränsningar på demoversionen, vilket påverkade resultaten en del.

## 7 REFERENCES

ABB Oy, 2007. *REK 510 - User's manual*, Vaasa: ABB Oy.

ABB, 2019. *Generator Protection and Control REG630 Application Manual*, s.l.: s.n.

Ahmad, M., 2018. *Operation and control of renewable energy systems*. Hoboken: John Wiley & Sons Ltd.

Arcteq, 2018. *AQ-G257 Generator protection IED Instruction manual*, s.l.: s.n.

Atienza, E. & Moxley, R., 2011. *Improving Breaker Failure Clearing Times*, Dublin: s.n.

Bathia, S. C., 2014. *Advanced Renewable Energy Systems*. New Delhi: Woodhead Publishing India PVT Ltd..

Bender GmbH & Co. KG, n.d. *Technical paper: Electrical safety for mobile generators*, s.l.: s.n.

Boldea, I., 2016. *Synchronous Generators*. 2nd ed. Miami: Taylor & Francis Group.

Breeze, P., 2018. *Hydropower*. London: Academic Press.

Breeze, P., 2019. *Power Generation Technologies*. San Diego: Elsevier Science & Technology.

DIgSILENT. 2022a. *PowerFactory 2021 (SP3, Demo)*. [Software]. [Accessed 31 March 2022]

DIgSILENT, 2022b. *PowerFactory 2022*, Gomaringen: DIgSILENT GmbH.

ETAP, 2020. *A Unified Digital Twin Platform*, Irvine: s.n.

ETAP. 2022. ETAP (Version 21, Demo). [Software]. [Accessed 29 April 2022]

Ferguson, C., 2016. *You are here: Home / Smart Grid / Generation / Generator Motoring: What It Is and How to Protect Against It.*, s.l.: JMK Engineering.

Fingrid Oyj, 2018. *Voimalaitosten järjestelmätekniiset vaatimukset VJV2018*, s.l.: s.n.

Fingrid Oyj, 2020. *Frequency quality analysis 2019*, s.l.: s.n.

Francisco Díaz-González, F., Sumper, A. & Gomis-Bellmunt, O., 2016. *Energy Storage in Power Systems*. Chichester: Wiley.

Hamududu, B. & Killingtveit, A., 2012. Assessing Climate Change Impacts on Global Hydropower. *Energies 2012*, Volume 5, pp. 305-322.

IEA, 2011. *2011*. [Online] [Accessed 10 February 2021].

IEA, 2020. *Hydropower*. [Online] [Accessed 4 February 2021].

IEEE, 2007. *IEEE Guide for AC Generator Protection*. New York: IEEE.

Le, K. H. & Vu, P. H., 2019. *Performance Evaluation of a Generator Differential Protection Function for a Numerical Relay*, s.l.: s.n.

López, M., Platero, C., Mayor, P. & R, G., 2017. *Review of Loss of Excitation Protection Setting and Coordination to the Generator Capacity Curve*, s.l.: s.n.

Mörsky, J., 1992. *Relesuojaustekniikka*, Hämeenlinna: Otatiето Oy.

Mowat, D., 2010. *Callide C Power Stations Generator Protection System “ride through capabilities” for various external faults*, s.l.: University of Southern Queensland Faculty of Engineering and Surveying .

NERC, 2015. *Considerations for Power Plant and Transmission System Protection Coordination* , s.l.: s.n.

Schmutz, S. & Sedzimir, J., 2018. *Riverine Ecosystem Management*. Cham: Springer Nature.

Schneider Electric, 2005. *Calculation of short-circuit currents*, s.l.: s.n.

Schneider Electric, 2017. *Easergy P3G30, P3G32 Generator Protection with Machine Differential Protection User Manual*, s.l.: s.n.

Schneider Electric, 2018. *VAMP 210 Generator Protection Relay User Manual*, s.l.: s.n.

Siemens, 2020. *SIPROTEC 5 Generator Protection Manual*, s.l.: s.n.

Siemens, 2021. *PSS®CAPE Protection Simulation Software*, Nuremberg: Siemens AG .

Siemens. 2022. PSS®CAPE (CAPE 15, Demo). [Software]. [Accessed 2 May 2022]

Thomas, D. T., 1972. *Engineering electromagnetics*. New York: Pergamon Press.

VELCO, 2013. *Glossary of electric system terms*. [Online] Available at: <https://www.velco.com/about/learning-center/glossary> [Accessed 15 March 2021].

Warne, D. F., 2005. *Newnes Electrical Power Engineer's Handbook*. 2nd ed. Great Britain: Elsevier.

## APPENDICES

**Appendix 1. Calculations of conversion between PQ-plot and RX-plot (NERC, 2015).**

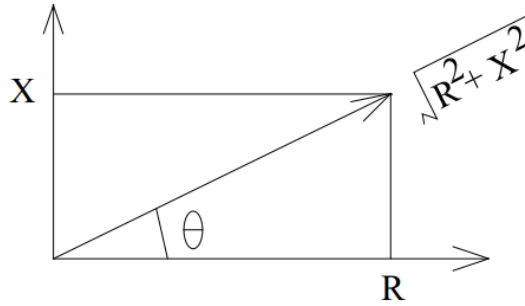
$$Q = \frac{X \cdot U_t^2}{R^2 + X^2}$$

$$P = \frac{R \cdot U_t^2}{R^2 + X^2}$$

$$X = \frac{Q \cdot U_t^2}{P^2 + Q^2}$$

$$R = \frac{P \cdot U_t^2}{P^2 + Q^2}$$

RX to PQ:



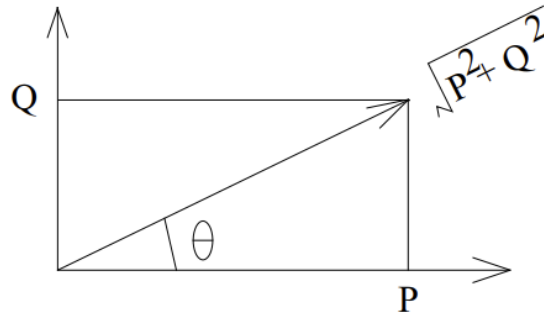
$$\cos\theta = \frac{R}{\sqrt{R^2 + X^2}}$$

$$S_{prim} = \frac{U_{LL,prim}^2}{Z_{prim}} = U_{LL,prim}^2 \cdot \left( \frac{CT_{RATIO}}{VT_{RATIO}} \right) \cdot \left( \frac{1}{Z_{sec}} \right)$$

$$P_{prim} = S_{prim} \cdot \cos\theta = U_{LL,prim}^2 \cdot \left( \frac{CT_{RATIO}}{VT_{RATIO}} \right) \cdot \left( \frac{R}{R^2 + X^2} \right)$$

$$Q_{prim} = S_{prim} \cdot \sin\theta = U_{LL,prim}^2 \cdot \left( \frac{CT_{RATIO}}{VT_{RATIO}} \right) \cdot \left( \frac{X}{R^2 + X^2} \right)$$

PQ to RX:



$$\cos\theta = \frac{P}{\sqrt{P^2 + Q^2}}$$

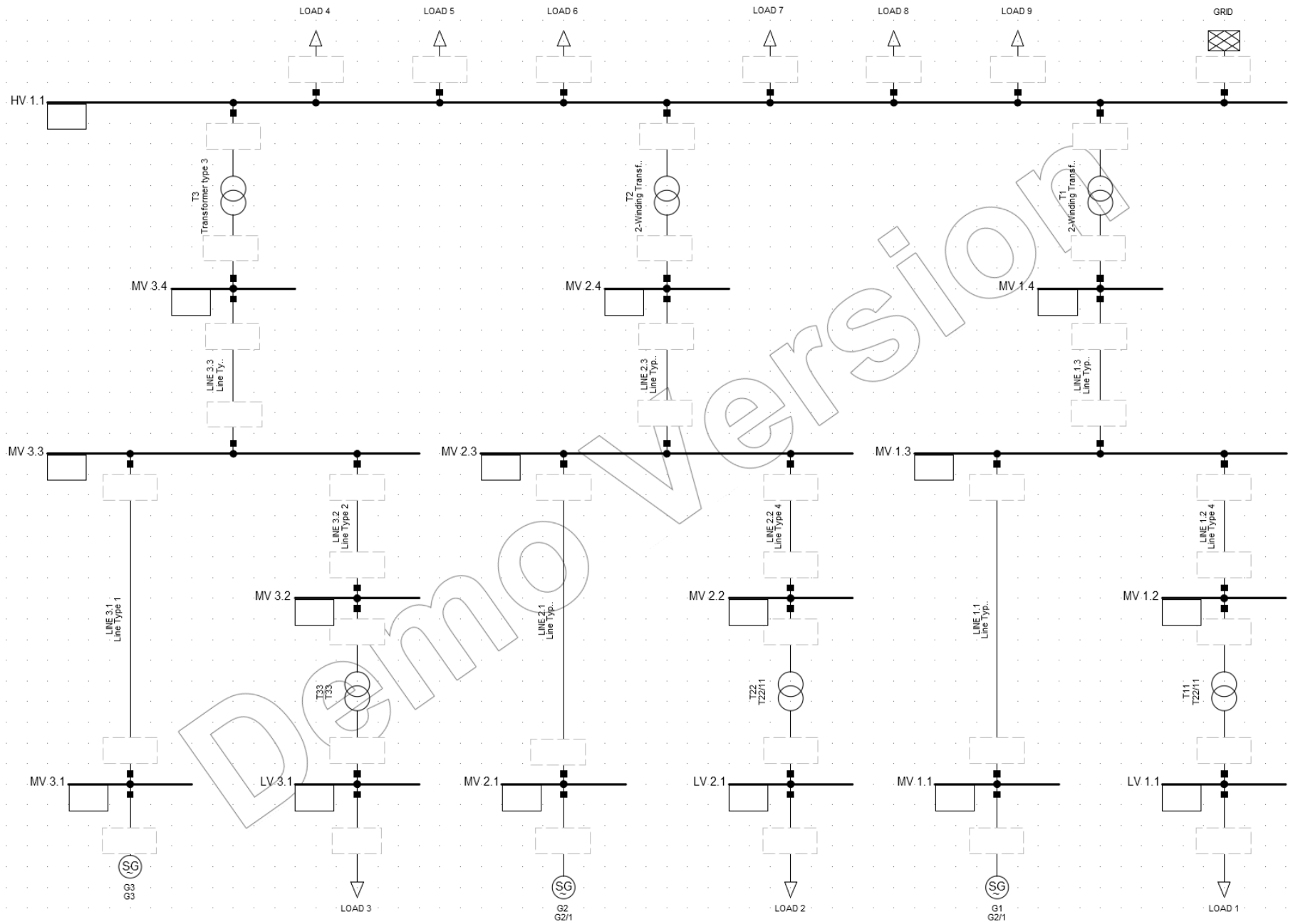
$$Z_{prim} = \frac{U_{LL,prim}^2}{S_{prim}}$$

$$Z_{sec} = Z_{prim} \cdot \left(\frac{CT_{RATIO}}{VT_{RATIO}}\right) = \frac{U_{LL,prim}^2}{\sqrt{P^2 + Q^2}} \cdot \left(\frac{CT_{RATIO}}{VT_{RATIO}}\right)$$

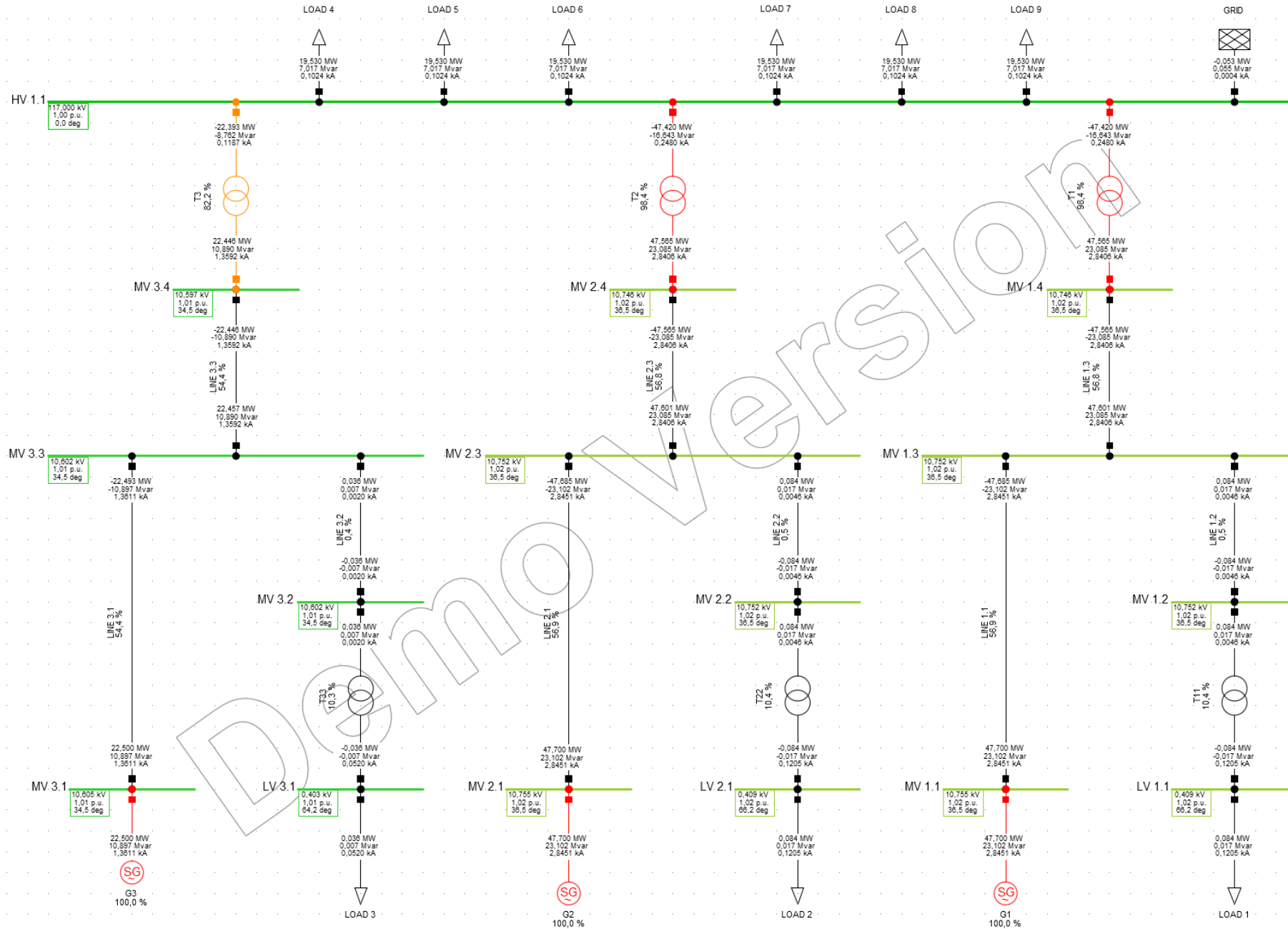
$$R_{sec} = Z_{sec} \cdot \cos\theta = U_{LL,prim}^2 \cdot \left(\frac{CT_{RATIO}}{VT_{RATIO}}\right) \cdot \left(\frac{P}{P^2 + Q^2}\right)$$

$$X_{sec} = Z_{sec} \cdot \sin\theta = U_{LL,prim}^2 \cdot \left(\frac{CT_{RATIO}}{VT_{RATIO}}\right) \cdot \left(\frac{Q}{P^2 + Q^2}\right)$$

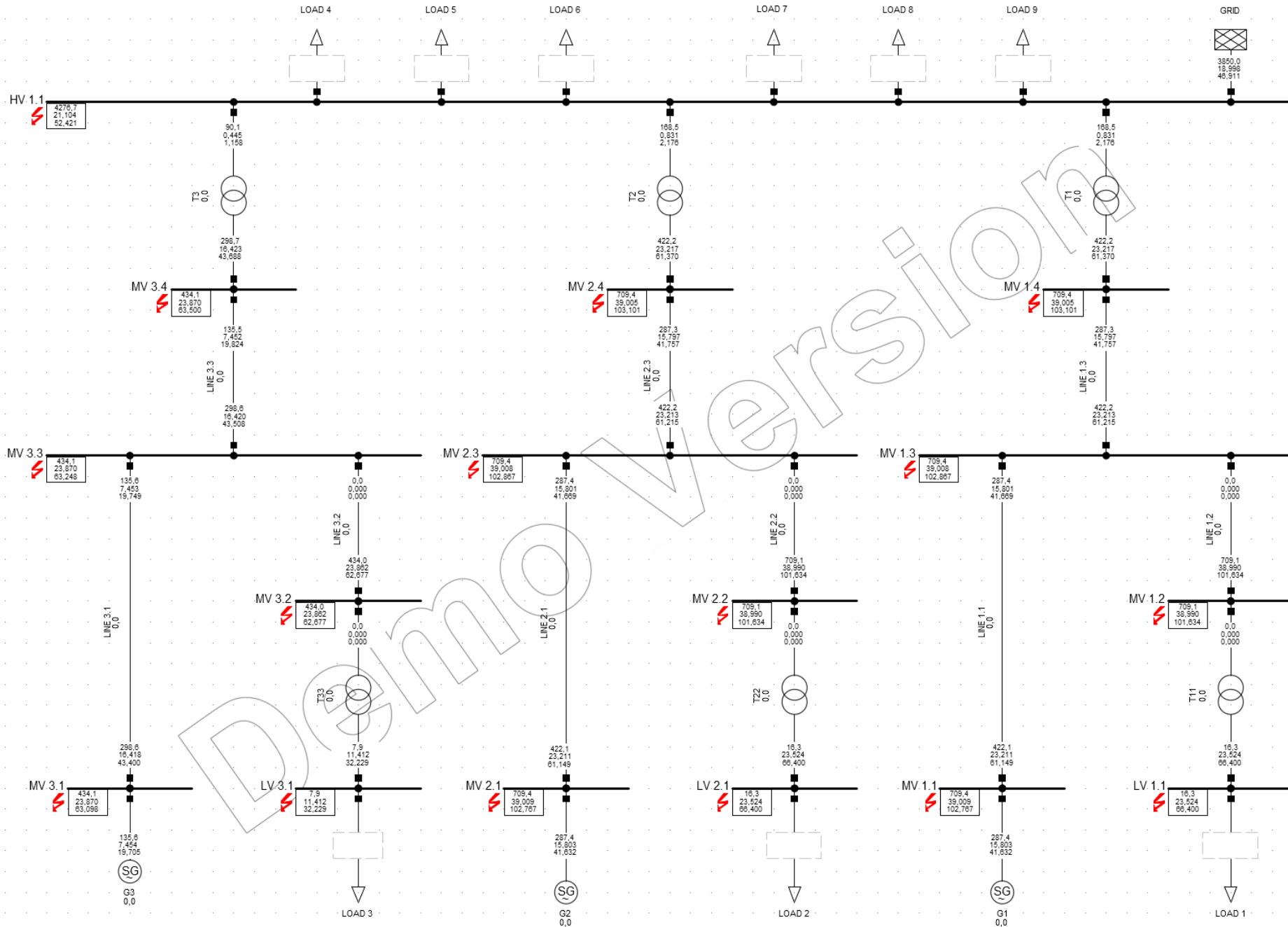
Appendix 2. The power plant design in Powerfactory Digsilent (Digsilent, 2022a; modified).



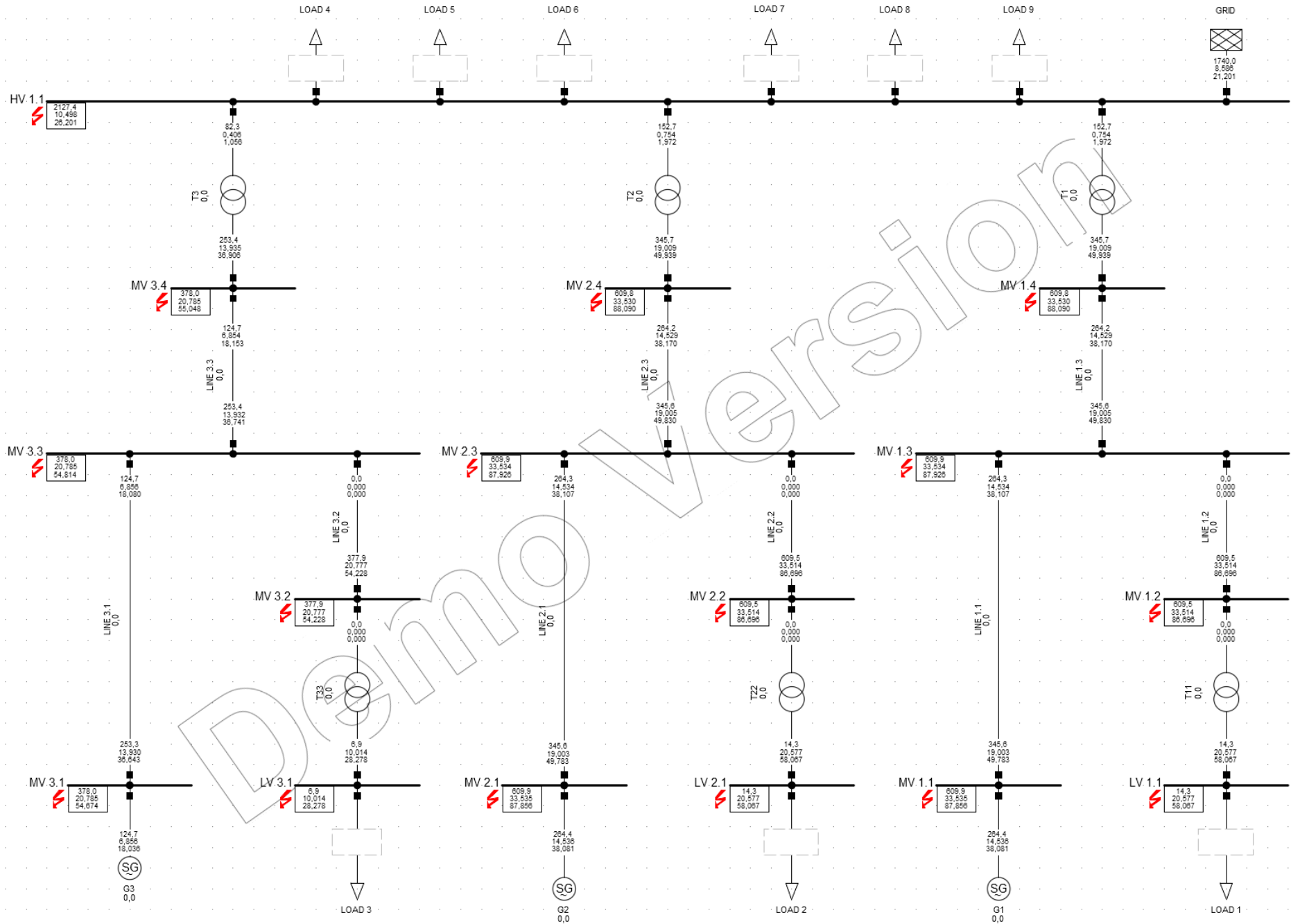
### Appendix 3. Load flow simulation in Powerfactory Digsilent (Digsilent, 2022a; modified).



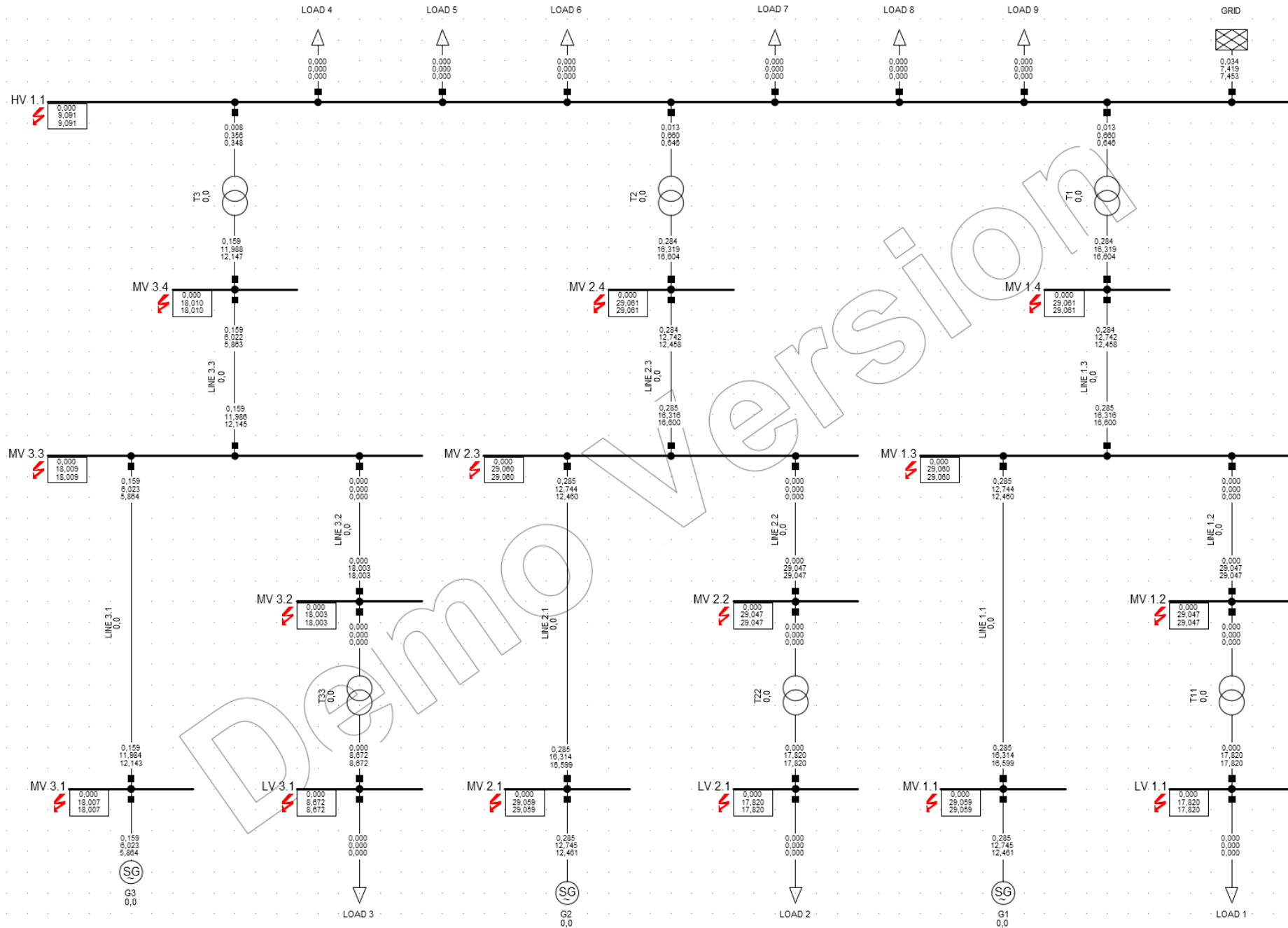
# Appendix 4. Maximum three-phase short circuit simulation in Powerfactory Digsilent (Digsilent, 2022a; modified).



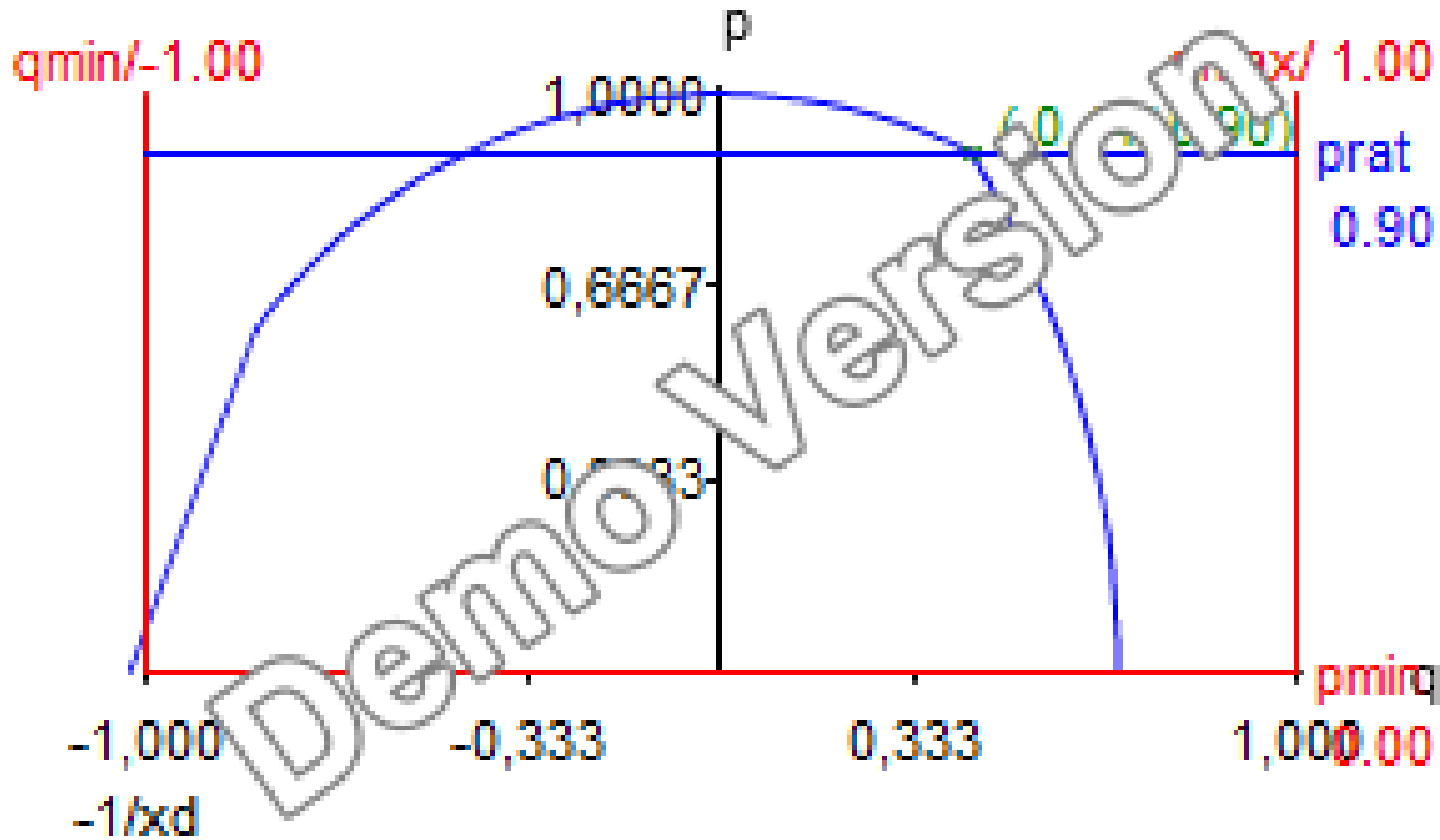
# Appendix 5. Minimum three-phase short circuit simulation in Powerfactory Digsilent (Digsilent, 2022a; modified).



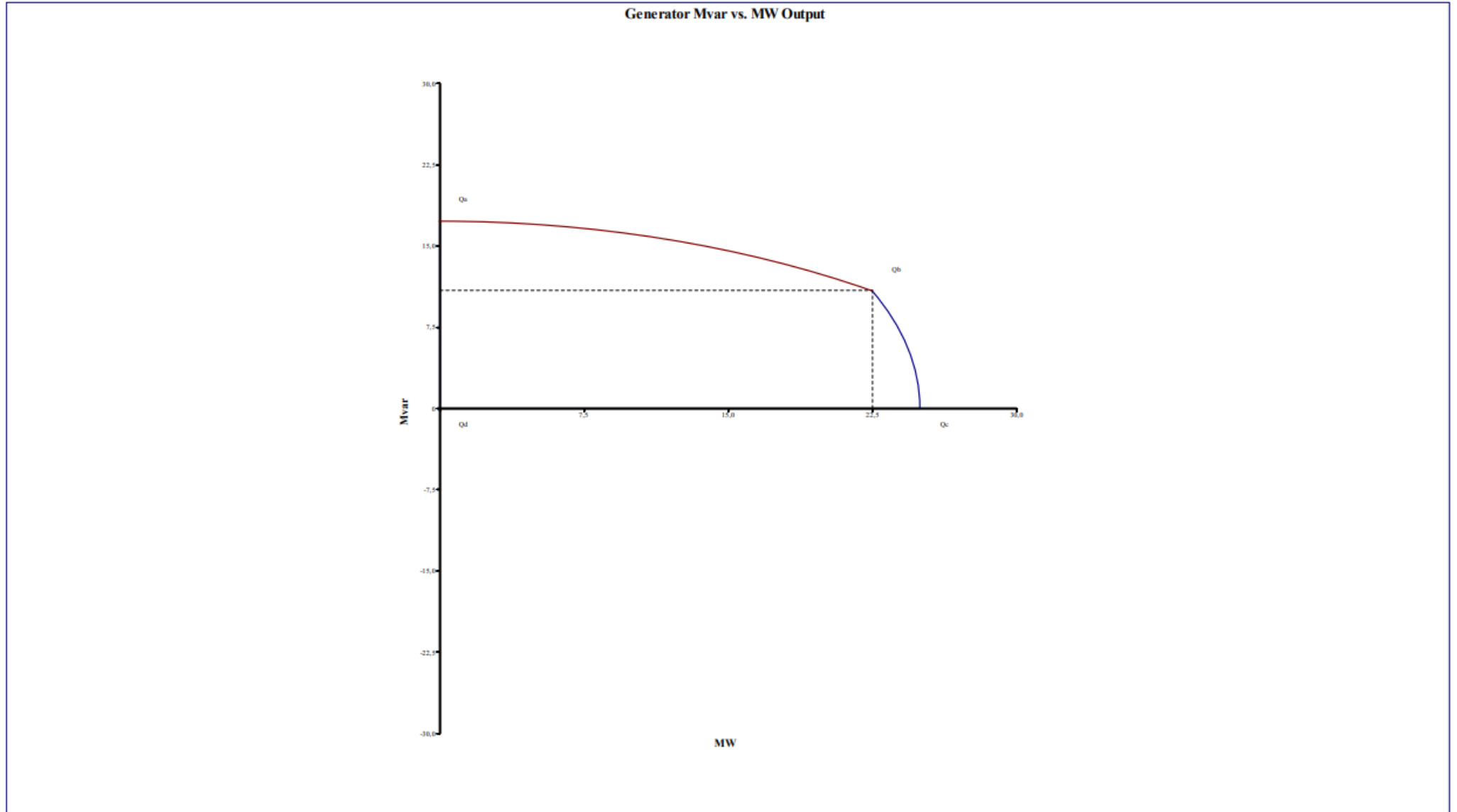
# Appendix 6. Minimum two-phase short circuit simulation in Powerfactory Digsilent (Digsilent, 2022a; modified).



Appendix 7. Illustration of the generator capability curve in Powerfactory Digsilent (Digsilent, 2022a; modified).



Appendix 8. Illustration of the generator capability curve in ETAP (ETAP, 2022; modified).



Appendix 9. Load flow simulation in Siemens PSS/CAPE (Siemens, 2022; modified).

